

EVENT DRIVEN SEDIMENT MOBILITY ON THE INNER
CONTINENTAL SHELF OF ONSLOW BAY, NC

Jeffery A. Marshall

A Thesis Submitted to the
University of North Carolina at Wilmington in Partial Fulfillment
Of the Requirements for the Degree of
Master of Science

Department of Earth Sciences

University of North Carolina at Wilmington

2004

Approved by

Advisory Committee

Dr. Lynn Leonard
Committee Co-Chair

Dr. Nancy Grindlay
Committee Co-Chair

Dr. Doug Gamble
Committee Member

Accepted by

Dr. Robert Roer
Dean, Graduate School

This thesis has been prepared in a style and format
consistent with
Marine Geology

TABLE OF CONTENTS

| | |
|--|------|
| ABSTRACT | v |
| ACKNOWLEDGEMENTS | vii |
| DEDICATION | viii |
| LIST OF TABLES | ix |
| LIST OF FIGURES | x |
| INTRODUCTION | 1 |
| STUDY AREA | 4 |
| Seasonal Hydrodynamic and Meteorological Conditions in Onslow Bay..... | 4 |
| Surficial Lithofacies in Onslow Bay..... | 4 |
| MATERIALS AND METHODS..... | 9 |
| Hydrodynamic Data Acquisition | 9 |
| Sidescan Sonar Acquisition and Processing | 11 |
| Geological Data Acquisition..... | 14 |
| RESULTS | 14 |
| Distribution and Characteristics of Surficial Sediments..... | 14 |
| Seasonal Averages of Hydrodynamic and Meteorological Data | 20 |
| Determination of Sediment Mobility | 22 |
| Tidal Currents | 24 |
| Waves and Wind-driven Currents..... | 25 |
| High-energy Events Responsible for Sediment Mobility | 28 |
| Southerly Wind Event: June 6 - 11, 2003 | 30 |
| Extratropical Low and Frontal Passage: December 23 - 28, 2002 | 33 |

| | |
|---|----|
| Tropical Storm Gustav: September 7 - 12, 2002 | 37 |
| Hurricane Isabel: September 15 - 20, 2003 | 41 |
| Sidescan Sonar Change Detection Analysis | 44 |
| Coarse Sand Body One (CSB-1)..... | 46 |
| Fine Sand Body One (FSB-1)..... | 50 |
| Coarse Sand Body Two (CSB-2)..... | 52 |
| Fine Sand Body Two (FSB-2) | 54 |
| Fine Sand Body Three (FSB-3) | 55 |
| Fine Sand Body Four (FSB-4) | 55 |
| DISCUSSION..... | 57 |
| CONCLUSIONS..... | 68 |
| REFERENCES | 71 |
| APPENDICES | 74 |
| Appendix A..... | 74 |
| Appendix B..... | 76 |
| Appendix C | 82 |
| Appendix D..... | 84 |

ABSTRACT

This study seeks to further constrain near-bottom hydrodynamic current conditions required to mobilize native sediments on a high-energy sediment starved shelf environment and link these data to changes in sidescan sonar imagery of the inner-shelf environment of Onslow Bay, NC. A bottom-mounted upward looking Acoustic Doppler Current Profiler (ADCP) deployed at the OB3M study site on the lower sand flat adjacent to a low-relief marine hardbottom recorded hourly flow velocity profiles from a depth of 17.7 m. The lower sand flat is composed of two dominant surficial lithofacies consisting of patchy, but well-defined areas of well sorted fine sand and poorly sorted coarse grained material. A dual frequency high-resolution sidescan sonar system was utilized to biannually survey a 5.5 by 3.7 km area encompassing the OB3M site between March 2002 and October 2003. Mosaic imagery obtained from these surveys were used to document seasonal changes in bottom characteristics in response to twenty-three identified sediment mobility events. Measurable contributions from semidiurnal tidal flows, mean current flows dominated by subtidal wind-generated currents, as well as wave-generated oscillatory motions in the near-bottom layer during storm and non-storm conditions have been identified for the nineteen-month period bracketing two tropical storm seasons off the North Carolina coast. Calculated critical shear velocity values due to the combined effects of waves and currents indicate that the fine-grained sand fraction was mobile more than 66% of the period, frequently as incipiently suspended load and bedload, and rarely as fully suspended load. Quantitative analysis of sidescan sonar imagery demonstrate that even though hydrodynamic conditions favor mobilization of fine sands, the gross morphology and sediment distribution at this inner-shelf site remained relatively unchanged after the occurrence of several commonplace high-energy events. Seasonal sedimentation patterns, however; were found to be substantially altered after the passage of Hurricane Isabel within 225 km of the study site. Evidence from this

study reveals that over the nineteen-month study period at this discrete site, the combined effects of typical high-energy events had little effect on the net distribution of bottom sediments, yet a singular extreme event was found to actively modify seabed sedimentation processes.

ACKNOWLEDGEMENTS

I would like to first thank Dr. Lynn Leonard who encouraged and guided me through this project with unbridled enthusiasm and unending support. I would also like to thank and credit the remainder of my faculty committee, Dr. Nancy Grindlay and Dr. Doug Gamble, whose patience and thoughtful advice throughout this process led to the successful completion of this manuscript. I would like to further thank CORMP technicians Jay Souza, David Wells and Morgan Bailey, who were key in diving operations and general data acquisition required for this project. These gentlemen are true professionals and were a pleasure to work throughout the duration of our research.

I would also to acknowledge Doug Kesling and Ken Johns who provided me with the necessary diving skills needed to make this research truly tangible. Further thanks go to Capt. Gerry Compeau of the R/V Seahawk and the mates of the R/V Cape Fear, Mike Rodaway and Chuck Ruch, as well as John Moore who assisted with acquisition of sidescan sonar data. I would also like to thank Dr. Ansley Wren who provided welcomed insight, unwavering support and who along with Matt Head assisted in diving operations for this research.

This research was funded by the National Oceanic & Atmospheric Administration, Award # NA16RP2675. I would also like to thank the UNCW Graduate School and Department of Earth Sciences for their financial support of my research and studies.

DEDICATION

I would like to dedicate this manuscript to my loving family and friends. Without your unwavering support and constant encouragement none of this work would have been possible and for that I thank you.

LIST OF TABLES

| Table | Page |
|--|------|
| 1. Acoustic Doppler Current Profiler (ADCP) deployment dates for this study | 10 |
| 2. Seasonal near-bottom current flow data measured at 1.22 m above the bed (mab) | 21 |
| 3. Seasonal significant wave and acoustic backscatter signal (ABS) data obtained from the OB3M study site via an ADCP moored on the inner-shelf (17.7 m depth)..... | 23 |
| 4. Summary of four major sediment mobility events observed between April 25, 2002 and October 14, 2003 | 31 |
| 5. Displacement (m ²) and net direction of movement of selected subareas located on lower sand flat adjacent to marine hardbottom reef | 51 |
| 6. Conceptual model comparing area analysis of six subareas examined during biannual sidescan sonar results to frequency, distribution, and intensity of high-energy sediment mobility events..... | 61 |

LIST OF FIGURES

| Figure | Page |
|---|------|
| 1. Regional view of Onslow Bay and surrounding offshore waters | 5 |
| 2. Site map of Onslow Bay lower shoreface and inner continental shelf study area | 6 |
| 3. OB3M site bathymetry and sidescan sonar track lines | 7 |
| 4. Sidescan mosaic of the regional area surrounding the OB3M study site acquired March 2002 using the 100 kHz frequency channels | 13 |
| 5. Generalized bottom type map of OB3M inner-shelf study site corresponding to mosaic imagery provided in Fig. 4 | 16 |
| 6. Sidescan image of marine hardbottom reef area and lower sand flat displaying dominant lithofacies at the inner-shelf site | 17 |
| 7. Digital photographs of gravelly coarse sand sediment type positioned on the lower sand flat..... | 18 |
| 8. Digital photographs of well-sorted fine sand sediment type located on lower sand flat..... | 19 |
| 9. Time-series of burst averaged parameters demonstrating subtidal current response at 1.22 mab from May 20 - 25, 2002 | 27 |
| 10. Southerly wind event sediment mobility evidence | 34 |
| 11. Evidence for sediment mobility from December 25, 2002 extratropical low | 36 |
| 12. Tropical Storm Gustav sediment mobilization evidence | 39 |
| 13. Hurricane Isabel sediment mobility evidence..... | 42 |
| 14. Location of 6 subareas where change detection analysis was performed using biannual sidescan (100 kHz) surveys | 45 |
| 15. Ten meter error buffer surrounding subarea sand bodies located on the lower sand flat where change detection analysis was performed | 47 |
| 16. Sand contact displacement results from CSB-2 spanning the period between March 2002 and October 2003 | 48 |

| | |
|---|----|
| 17. CSB-1 and FSB-1 sand body contacts | 49 |
| 18. CSB-2 and FSB-2 sand body contacts | 53 |
| 19. FSB-3 and FSB-4 sand body contacts | 56 |
| 20. Sediment relief peel produced from diver collected boxcore obtained approximately 30 m south of OB3M instrumentation cage | 64 |
| 21. Bar graph showing distribution of suspended sediment amounts obtained in a sediment cup positioned 23 cm above the seabed and mounted vertically to the OB3M instrumentation cage | 67 |

INTRODUCTION

A number of hydrodynamic processes responsible for mobilization of sediment on the lower shoreface and inner continental shelf have been identified and described (Grant and Madsen, 1979; Niedoroda et al., 1985; Wright et al., 1986; Wright, 1987; Wright, et al., 1991; Wright, 1995; Thielor, 1996; Xu and Wright, 1998). Tidal forces and the currents produced in response to astronomical forces are the best understood and most predictable of the physical forcing mechanisms initiating sediment mobilization on the inner continental shelf (Wright, 1995). Tidal oscillations and the resulting flows consist of a number of diurnal, semidiurnal, and longer period constituents, each of which is a response to forcing terms of varying frequency and magnitude. The most influential of these partial tide constituents is the M2, main lunar semidiurnal with a period 12.42 hours. Wright et al. (1991) and Wright et al. (1993) noted in recent research along the lower shoreface of Duck, NC that tidal currents are generally weak (maximum of 10-20 cm s⁻¹ during spring tides) and individually have little significance in initiating sediment activity. However, when combined with bed agitation by wave orbital and wind driven flows, tidal forces contribute to the overall shear stress on the seabed which aids in transporting sediment across and along the shelf (Wright et al., 1991; Wright et al., 1993).

Low frequency wind-driven southerly currents produced most often in response to nor'easter type storms have been observed on the inner-shelf to be significant mechanisms responsible for sediment mobility. In addition to strong near-bottom along-shelf currents, these flows also have the ability to produce mesoscale across-shelf downwelling flows reaching velocities greater than 10 cm s⁻¹ (Wright et al., 1986; Wright, 1995). During study on the mid-Atlantic Bight inner-shelf, which included only moderate energy storms, offshore and alongshore transport of sediment was noted in response to these elevated bottom currents (Wright et al.,

1986). Offshore of Wrightsville Beach, North Carolina much of the observed across-shelf transport is also hypothesized to be accomplished during storms by enhanced bottom stresses brought on by downwelling currents due to storm set-up, in conjunction with above average wave-induced oscillatory flows (Thieler et al., 1999).

By far, the primary means of initiating sediment mobility in the inner-shelf environment is through surface gravity wave orbital motions translating vertically through the water column and interacting with the seafloor (Wright et al., 1991). In all cases, the effects of incident waves were the most significant processes leading to the mobilization of sediment as bedload and suspended load, but could be either positively or negatively influenced by the other physical processes occurring simultaneously during varying energy climates (Wright et al., 1991). Additional work by Wright et al. (1994) specifically focused on sediment dynamics during the extremely unique severe and prolonged Halloween Storm, which battered much of the eastern seaboard during late October 1991. These data again demonstrated a strong relationship between wave orbital oscillations, mean current flows and wave-current interactions on sediment suspension fluxes and allowed the authors to better constrain the relative contributions of these processes to sediment transport under a given set of meteorological and oceanographic conditions.

In Onslow Bay off the North Carolina coast, it is well established that the near-bottom processes that produce along-shelf and across-shelf sediment transport are more powerful during storms than during fair-weather periods (Renaud et al., 1996, 1997); Schmid, 1996; Riggs, et al., 1998; Wren and Leonard, 2004). High-resolution seafloor bottom mapping and post-storm video obtained after extreme storms at inner and mid-shelf (< 30 m depth) sites within Onslow Bay have demonstrated significant changes in surficial sediment distribution, of which the authors

have attributed as a direct response to storm induced currents (Renaud et al., 1996; Riggs et al., 1996; Renaud et al., 1997; Riggs et al., 1998; Thieler et al., 2001). Several of these studies centered on storm events that were the largest magnitude on record for this region and may not be indicative of conditions associated with events that are more commonplace. In each of these studies, bottom conditions associated with the events were based on short-term current meter moorings or estimated from hindcasted wave data obtained considerable distances from the actual location. Thus, a true picture of the effects of storms on hydrodynamic conditions and sediment mobility in the near-bottom layer were still lacking until very recently.

This present paper seeks to further refine knowledge of near-bottom hydrodynamic current conditions required to mobilize native sediments on a high-energy sediment starved shelf environment and to link these data to changes observed in repeat sidescan sonar surveys of the region. Specifically, contributions from tidal and subtidal current flows, as well as wave-generated oscillatory motions in the near-bottom region of the seabed during storm and non-storm conditions have been identified and quantified for the nineteen-month period bracketing two tropical storm seasons off the North Carolina coast. To further constrain the hydrodynamic conditions under which sediments are mobilized, associated meteorological surface conditions during periods of significant sediment mobility have been identified and grouped into a broad system of classification. Sidescan sonar imagery will demonstrate that even the passage of weak tropical systems and high-energy winter storms (nor'easters) over this period have not effectively transported widely distributed, fine-grained bottom sediment across the seabed, even though hydrodynamic conditions warrant sediment redistribution. Data presented in this paper stem from research conducted under the support of the Coastal Ocean Research and Monitoring Program (CORMP). This multidisciplinary program of study investigates and monitors the

physical, geological, chemical, and biological processes occurring on the continental shelf in the South Atlantic Bight.

STUDY AREA

Onslow Bay is located off the coast of southeastern North Carolina (Fig. 1). It is a broad, shallow embayment bounded to the northwest by Cape Lookout, to the southwest by Cape Fear, and eastward by the continental slope break located along the approximately 100 m depth contour. The inner continental shelf location chosen for this study is positioned in water depths of 15-17 m approximately 8 km east of Masonboro Island, transgressive barrier island (Fig. 2).

Seasonal Hydrodynamic and Meteorological Conditions in Onslow Bay

Mean tidal range is approximately 1.0 m, placing the location in a microtidal setting as defined by Hayes (1979). It is also a high-energy, wave-dominated environment yielding average significant wave heights, as calculated by an *in-situ* ADCP over the nineteen-month study period, of 0.9 m and average dominant wave periods of approximately 7.3 seconds. These data agree well with other locally performed wave climate studies (Jarrett, 1977) and regionally calculated hindcast data (WIS research). Wave approach at this location is seasonally dependent. In winter, the dominant wave approach is from the northeast, and in summer this direction typically reverses to the southeast. Further, waves originating to the south as well as east are not uncommon, especially during the passage of tropical cyclones and extratropical storms (Thieler et al., 1995; Thieler et al., 2001).

Surficial Lithofacies in Onslow Bay

The OB3M study site (known locally as Five Mile Ledge) is located adjacent to a low-relief rock outcrop in Onslow Bay, NC, at an average depth of approximately 17.7 m (Fig. 3).

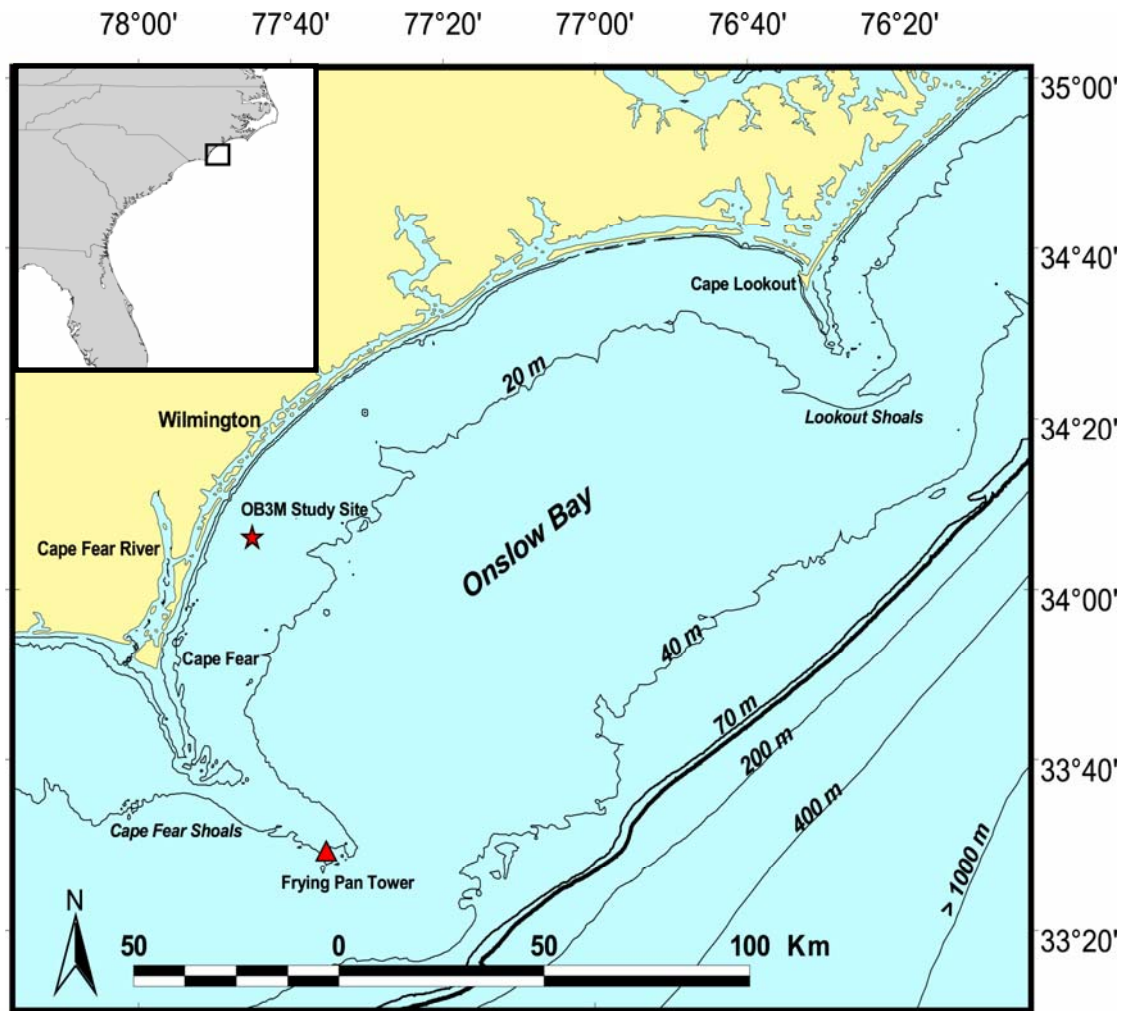


Fig. 1. Regional view of Onslow Bay and surrounding offshore waters. Onslow bay is bordered to the northeast by Lookout Shoals and Raleigh Bay and to the southwest by the Cape Fear Shoals and Long Bay. Instrumentation deployed for this study were located at OB3M. Frying Pan Tower marks the NOAA C-Man station where wind data were collected. The 100 m bathymetric contour (boldfaced) indicates location of the continental shelf break.

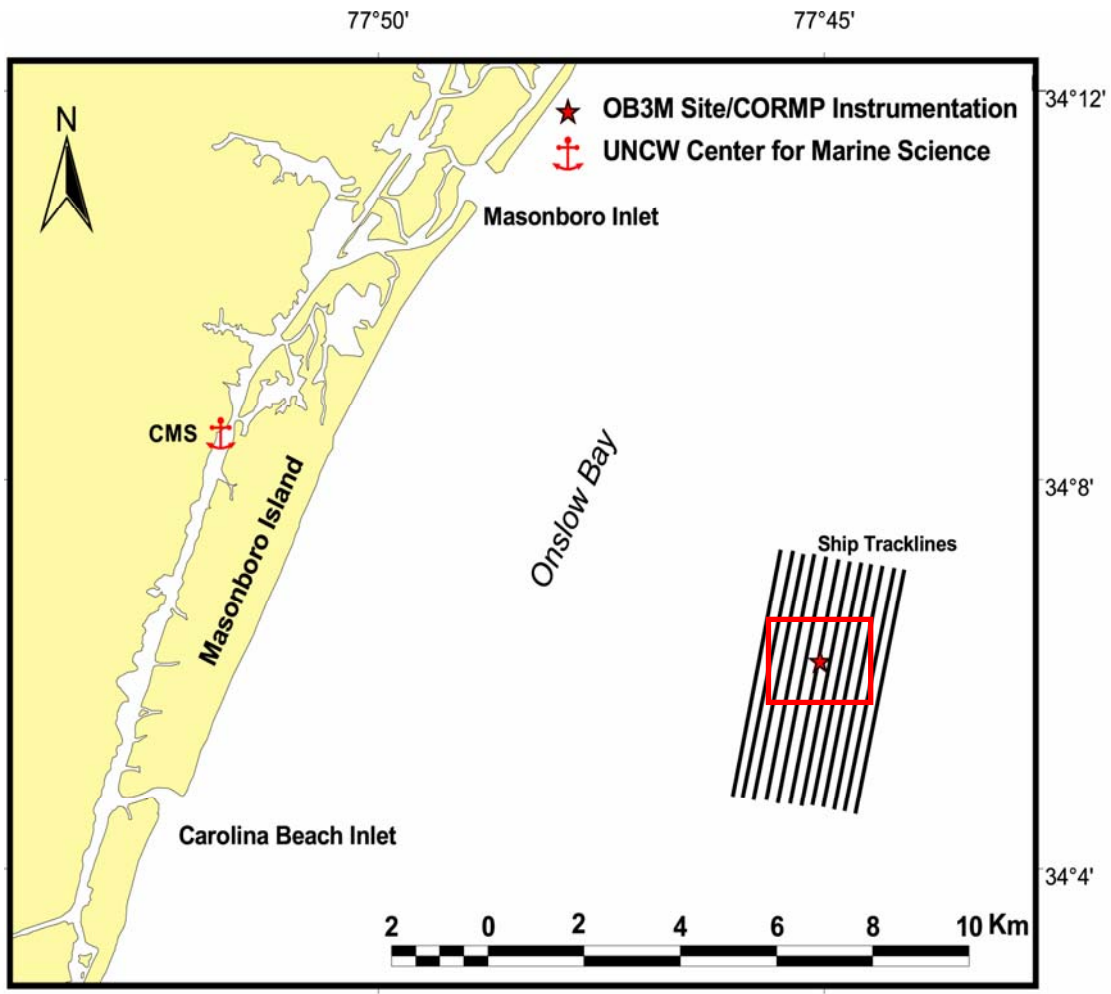


Fig. 2. Site map of Onslow Bay lower shoreface and inner continental shelf study area. Ship track lines used for sidescan sonar survey are also provided. Sidescan swaths cover 100 m on each side of the track lines and run northeast to southwest for approximately 5.5 km. Bathymetry data for the immediate area surrounding the OB3M instrument site (red box) is given in Fig. 4.

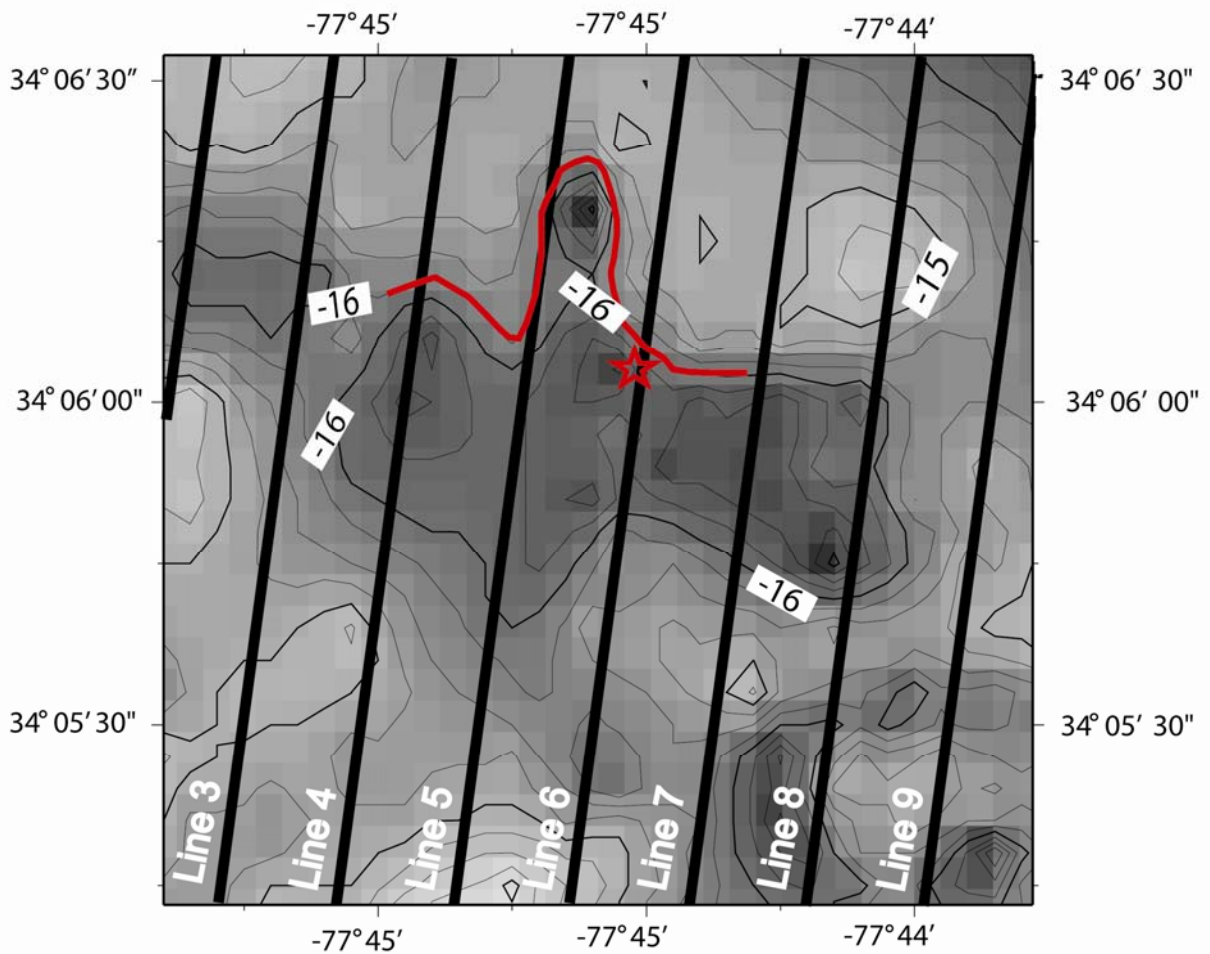


Fig. 3. OB3M site bathymetry and sidescan sonar track lines. Bathymetry is contoured using 0.25 m intervals and labeled every 1 m. Sidescan swaths cover 100 m on each side of the track lines. Approximate locations of the marine hardbottom reef ledge (red line) and ADCP instrument site (star) are also provided.

Exposed outcrops, commonly termed marine hardbottoms, are not uncommon in Onslow Bay as it is starved of major sediment input due to trapping of local riverine sediments in back barrier marshes (Blackwelder et al., 1982). Further, it is isolated from adjacent embayments by two major capes and associated shoals, thereby limiting alongshore exchange of sediment (Blackwelder et al., 1982). The modern unconsolidated sediments that do exist on the lower shoreface and inner-shelf seabed result from three major inputs. The surficial sediment cover has been categorized as residual, ultimately resulting from the erosion of underlying relic sediments and rocks (Milliman et al., 1972). Further, native sediments in this region have accumulated via shoreface bypassing of the underlying relict Oligocene aged unconsolidated sediments (Thieler et al., 2001) as well as through the physical and bio-erosion of exposed live reef hardbottoms prevalent across the lower shoreface and inner-shelf (Riggs et al., 1996; Thieler et al., 1995; Thieler et al., 2001). Additionally, beach replenishment of nearby Wrightsville Beach has been identified by Pearson and Riggs (1981) and Thieler et al. (1999, 2001) to have exceeded natural limits, and this “extra” sediment has proceeded to leak offshore and be deposited onto portions of the lower shoreface and inner-shelf.

Aside from the abundant marine hardbottoms, two distinct surficial lithofacies dominate the inner and mid-shelf landscape. Poorly sorted gravelly sands exist as lag pavement in topographic depressions adjacent to higher relief hardbottom areas and ancient erosional scarps (Riggs et al., 1996; Riggs et al., 1998). This gravelly coarse sand fraction is believed to be derived primarily from the bioerosion of numerous Plio-Pleistocene aged rock outcrops and biogenic material accompanying hardbottom reef areas (Thieler et al., 1995). As described by Renaud et al. (1997) and Riggs et al. (1998), well-sorted fine sands comprise the second distinct bottom type and occur in four general locales within Onslow Bay. The first two occurrences of

these fine sand areas are sand aprons and sand ramps immediately adjacent to the perimeter of hardbottom areas. The third occurrence is away from the hardbottom, in what are known as the lower sand flats, where thin, discontinuous sheets bury the gravel-based sand dunes. Locally, the vertical breadth of these fine sand bodies has been measured to be extremely thin, averaging 30 cm in most places (Thieler et al., 1995). Lastly, thin veneers (< 5 - 25 cm) of very fine to silty sands that have been suspended and later redeposited within fractures or depressions among the flat hardbottom also occur (Riggs et al., 1998). Fine sand bodies are hypothesized to primarily be a product of shoreface bypassing of underlying relict Oligocene units composed of silts to fine grained sands (Thieler, et al., 1995; Thieler et al., 2001). A third transitional facies has also been identified at mid-shelf locales along the boundaries of the fine and gravelly coarse sand bodies where the sediment types intermix (Schmid, 1996).

MATERIALS AND METHODS

Data collection occurred from March 2002 through October 2003 (Table 1) and utilized two distinct methods of collection: 1) continuous hydrodynamic time-series data collected by moored instrument packages; and 2) sediment cores, grab samples and sidescan imagery collected periodically prior to and following significant storm events.

Hydrodynamic Data Acquisition

All hydrodynamic data were collected at the OB3M study site (34° 06.13 N, 77° 45.05 W) shown in Figs. 2 & 3. An aluminum cage moored to the seafloor via sand screws at OB3M housed a 1200 kHz RDI Workhorse Sentinel Broadband Acoustic Doppler Current Profiler (ADCP) initially deployed in spring 2002. A crescent-shaped hardbottom with relief of approximately 1.5 m bounds the northern and western sides of the moored instrumentation at the OB3M study site, which sits approximately 30 m due west of the reef ledge. Similar to the

Table 1. Acoustic Doppler Current Profiler (ADCP) deployment dates for this study. Also noted are sidescan sonar survey acquisition dates.

| Season | Deployment Period | Sidescan Survey Date |
|------------------|-----------------------------|-----------------------------|
| Spring 2002 | 4/25 - 6/21 | 3/14/02 |
| Summer 2002 | 6/21 -7/10; 7/24 -10/14 | - |
| Fall 2002 | 7/24 -10/14; 10/29 -1/14 | 11/21/02 |
| Winter 2002-2003 | 10/29 -1/14; 1/17 -4/11 | - |
| Spring 2003 | 1/17 - 4/11; 4/20 - 7/11 | 5/30/03 |
| Summer 2003 | 4/20 - 7/11; 7/20 -10/10 | - |
| Fall 2003 | 7/20 -10/10; 10/24 -1/14 | 10/14/03 |

remainder of the gently sloping shelf of Onslow Bay, the bathymetry surrounding the instrumentation site is extremely gradual (Fig. 3).

The upward looking ADCP collected current velocity data through the water column in 0.70 m bins beginning at a height of 1.2 m off the seabed (mab) using a 2 Hz ping rate for 3600 seconds (one ensemble) every 60 minutes. The ADCP also possessed wave gauge capabilities that recorded wave period, significant wave height, average water depth to sensor, and significant wave direction. Wave data were recorded at a 2 Hz ping rate for 1200 seconds every four hours. Velocity time series data from the 1.2 m bin height above the bed were used when investigating near-bottom conditions and calculating bed shear velocity.

The ADCP instrument was configured for deployment durations of 10 -12 weeks and was retrieved by divers utilizing SCUBA aboard the R/V *Seahawk* and R/V *Cape Fear*. Typical turn around time between successive deployments averaged less than one week (Table 1). Quality current data were retrieved on each of the deployments utilized for this study; however, wave data from the spring 2003 deployment are sporadic and inconsistent due to unknown reasons.

Relative suspended sediment concentrations were estimated at a height of approximately 1.2 mab using the raw acoustic backscatter signal (ABS) provided by the ADCP. Calibration techniques and methodology supplied by the RDI company allow for an accurate estimation of the absolute backscatter in units of decibels to be calculated (Deines, 1999). The ABS signal has been shown to be an acceptable proxy for estimating changes in suspended sediments and other particulate matter in the water column (Williams and Ross, 2001; Wren and Leonard, 2004).

Sidescan Sonar Acquisition and Processing

High-resolution sidescan sonar imagery was used to relate hydrodynamic conditions to seafloor geomorphology and analyze spatial changes in seafloor geomorphology due to high-

energy events. Four bi-annual sidescan sonar surveys centered upon the OB3M study region and covering an area of approximately 5.5 km by 3.7 km were conducted (Figs. 2 & 3). These surveys took place March 2002, November 2002, May 2003, and October 2003 (Table 1). The sidescan sonar data were collected with an EdgeTech DF1000 dual frequency digital towfish (100 and 500 kHz) using a range of 100m (200m swath width). This study uses the sonar imagery collected by the 100kHz channels. Twelve track lines were established in a north-south direction and bounded by the area 34° 07.26 N, 77° 45.47 W in the northwest and 34° 07.06 N, 77° 44.10 W in the southeast. Track line spacing was 200 m to ensure maximum seafloor coverage (Fig. 3). For this study, navigation was collected from a Nobeltec differential global positioning system (DGPS) with an accuracy of ± 3 -5 m. Further error in navigation may result from uncertainty of the towfish position in the water column at any given time and resulted in a total navigational error between ± 5 -10 m during this study.

The Isis Sonar v.6 software package distributed by Triton Elics International (TEI) was used for acquisition and processing of the sidescan sonar data. A sonograph is a product of the intensity of acoustical backscatter, which is displayed as a gray-scale image with pixel values ranging from 0 to 255. In this study, a reversed gray-scale was used. The highest backscatter intensities are displayed as 0 and lowest intensities as 255 (Fig. 4). The TEI Isis software package was used to make geometric and radiometric corrections during the processing of the raw acoustic data on a line-by-line basis. Individual lines were visually inspected and enhanced using the time varying gain (TVG), balance, and bottom track options to remove errors due to slant range, striping, beam pattern, and other effects degrading the image. Lines were processed at a base resolution of 0.25 x 0.25 m per pixel and then exported into the TEI Delphmap software package where they were mosaicked and georeferenced. Finally, the mosaics were fused into a

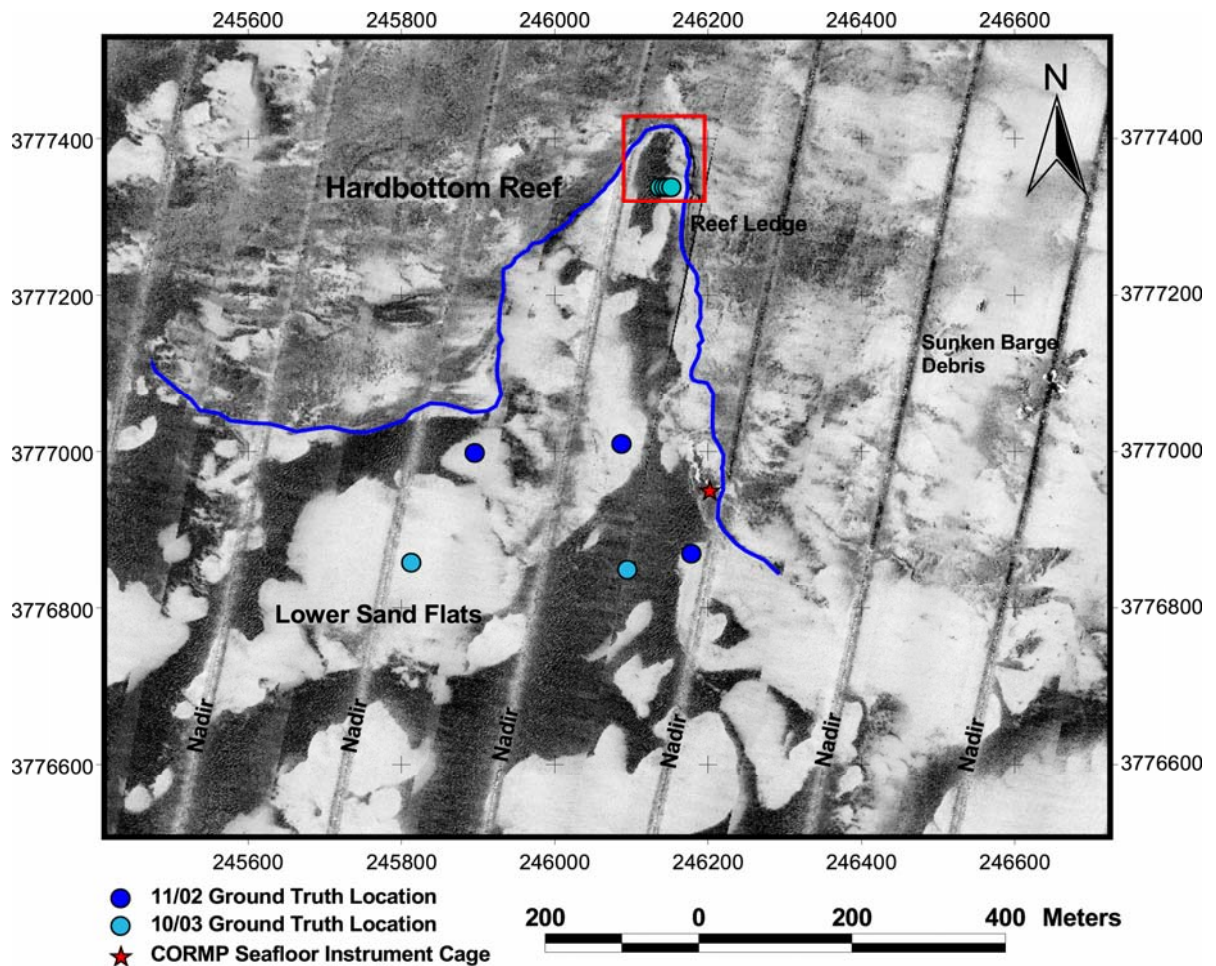


Fig. 4. Sidescan mosaic of the regional area surrounding the OB3M study site acquired March 2002 using the 100 kHz frequency channels. Pixel resolution is 0.25 x 0.25 m. Areas of high backscatter are displayed as dark returns and areas of low backscatter are observed as light returns. Grey-black lines trending northeast to southwest are the nadir region directly below ship track line corresponding to those given in Fig. 3. Marine hardbottom reef ledge is outlined in blue. The boxed area is enlarged in Fig. 6 and highlights surficial lithofacies common to the study area. Coordinates are eastings and northings and units are given in meters.

geographic information system (GIS) database using the ESRI ArcView 3.2 software package where the sidescan mosaic imagery could be further analyzed. Specific acquisition and processing parameters can be found in Appendix B.

Geological Data Acquisition

More than 40 boxcores were collected by divers utilizing SCUBA/NITROX under fair-weather conditions and after the occurrence of significant high-energy events within 30 m of the CORMP instrumentation cage. The cores, which penetrate the seafloor to a depth of approximately 30 cm, provide evidence of erosional and depositional sedimentary structures. Cores were sub-sampled at the core surface, approximately 5, 10, and 20 cm downcore for grain size analysis. Grain size characteristics were quantified using standard sieve techniques at one phi intervals. Relief peels, x-ray photographs, and digital photographs constructed from sediment cores were used to further describe broad scale external and internal sedimentary structure and bedding after techniques described by Beavers (1999). Over 30 surface grab samples were also collected and extensive visual observations were made pre- and post-sidescan surveys and during ADCP deployment and recovery to provide groundtruth for the sidescan sonar imagery.

RESULTS

Distribution and Characteristics of Surficial Sediments

The patchy, discontinuous placement of surface sediments across the inner-shelf seabed is well illustrated in a regional sidescan sonar mosaic image centered on the OB3M study site. Overall, the distribution of the major surficial sediment types is highly variable and is reflective of the limited availability of unconsolidated sediment (Fig. 4). In the immediate area

surrounding the OB3M site, mean grain size of the sediment ranges from 0.6 to 1.8 mm and composition is dominated by quartz, carbonate shell material, and small lithoclasts derived from the adjacent marine hardbottom area. A generalized bottom type map of the regional area surrounding the OB3M site and nearby marine hardbottom reef is given in Fig. 5 and illustrates the distribution pattern of the two major surficial lithofacies based on differences in mean grain size and sidescan sonar reflectivity patterns.

In the sidescan imagery, areas where gravelly coarse sands occupy the surface are delineated by regions of high backscatter, which are typically dark grey to black and have a striated appearance representing the megaripple type bedforms, which top them (Figs. 4 & 6). These poorly sorted sands are distinguished by the presence of long, straight megaripples, with measured wavelengths of 0.75 m and amplitudes of roughly 0.12 m and are believed to become mobilized under enhanced hydrodynamic conditions during storms (Thieler et al, 2001). In the immediate region surrounding the OB3M site, mean grain size of the coarse sands ranges from 0.6 to 1.8 mm, and composition is dominated by quartz, carbonate shell material, and small lithoclasts derived from adjacent marine hardbottom areas (Fig. 7).

Nearby areas of fine sands on the lower sand flat and atop the marine hardbottom are interpreted in sidescan imagery to be homogeneous areas of low backscatter, which typically appear as light grey to white in imagery mosaics (Figs. 4 & 6). Fine sands comprising also the lower sand flats adjacent to the OB3M instrumentation site exhibit a mean grain size between 0.19 - 0.22 mm and are well sorted, except for occasional shell fragments. Active three-dimensional ripples on the fine sand areas of the lower sand flats had wavelengths between 10 - 13 cm and amplitudes of roughly 5 cm as recorded by divers under fair-weather conditions (Fig. 8).

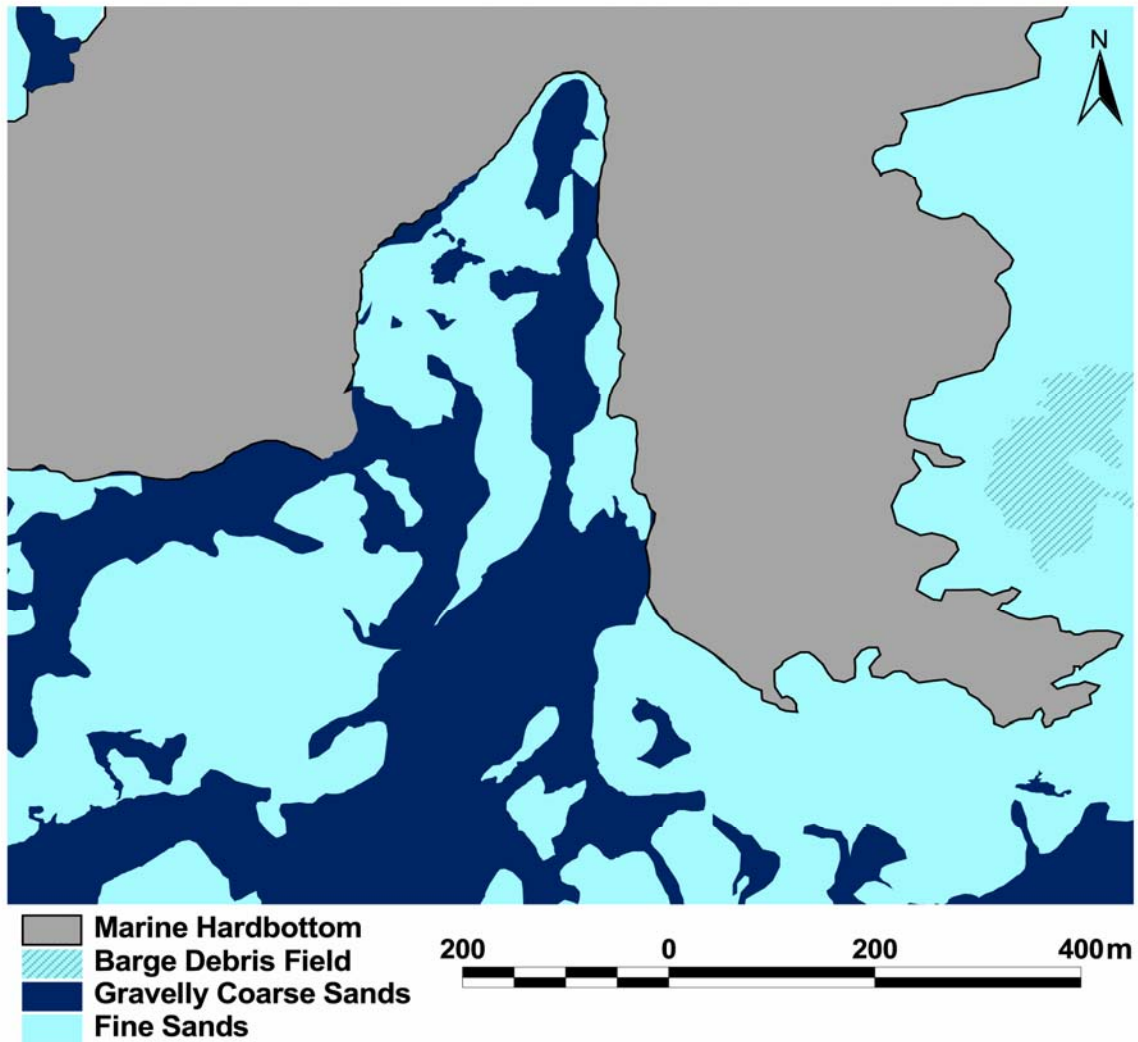


Fig. 5. Generalized bottom type map of OB3M inner-shelf study site corresponding to mosaic imagery provided in Fig. 4. Broad scale interpretation is based upon diver collected surface grab samples and sidescan sonar mosaic reflectivity patterns.

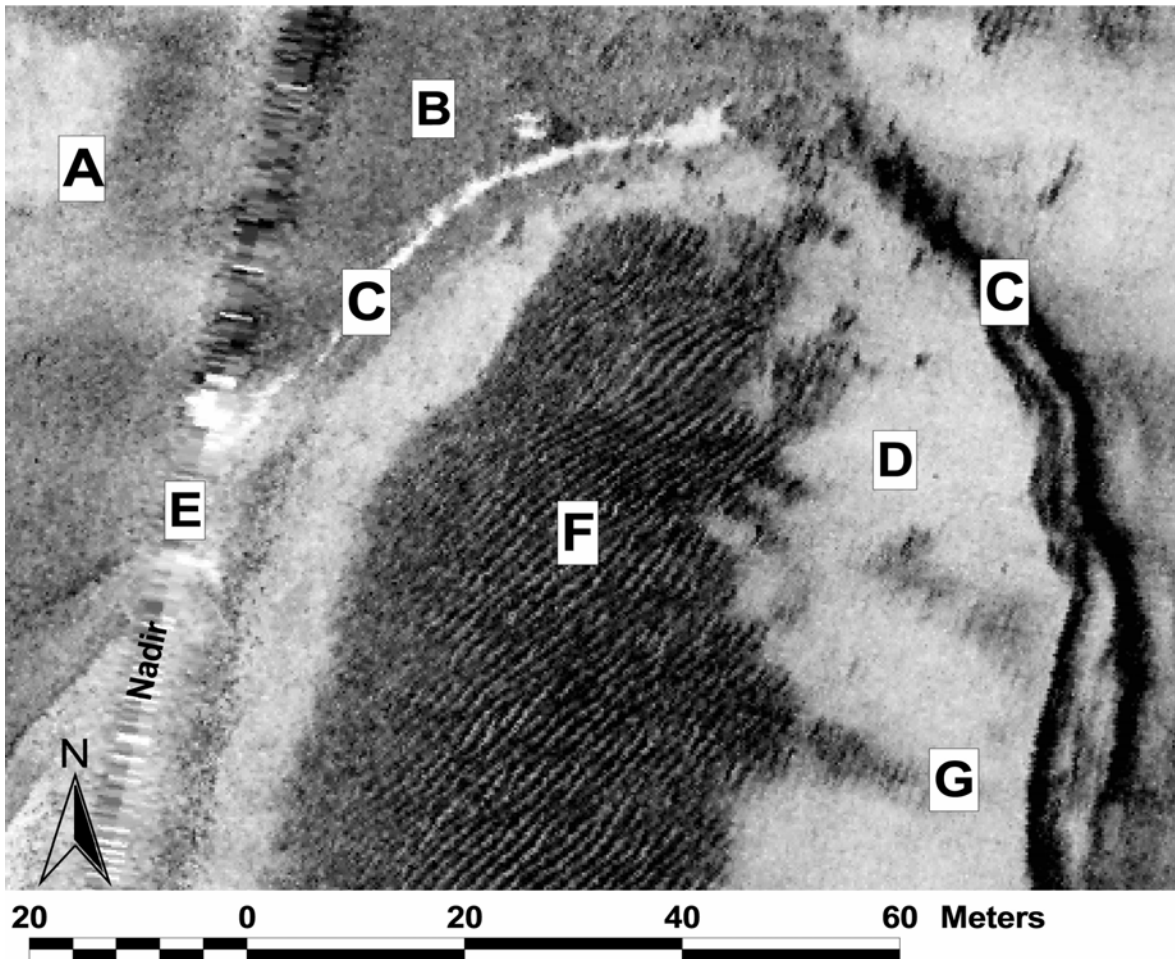


Fig. 6. Sidescan image of marine hardbottom reef area and lower sand flat displaying dominant lithofacies at the inner-shelf site. A = fine sand veneer atop hardbottom, B = exposed hardbottom with little to no sediment cover, C = reef ledge with adjacent fine sand sheet below, D = fine sand sheets overlying coarse gravelly sands demonstrating well-defined contact, E = sidescan sonar nadir, F = modern gravelly coarse sand composed of megaripples oriented to storm wave approach, G = area where fine sand sheet has been deposited over the pavement lag coarse sand as evidenced by long wavelength ripples showing through.

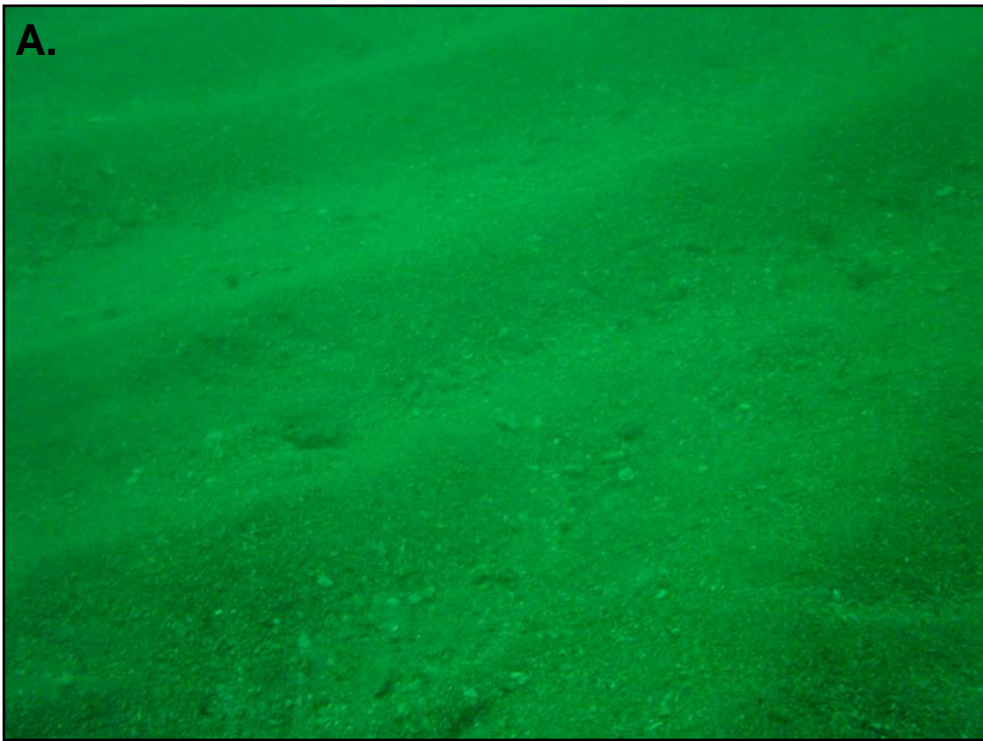


Fig. 7. Digital photographs of gravelly coarse sand sediment type positioned on the lower sand flat. Note the well-defined symmetric megaripples ($\lambda = 0.75$ m, $\eta = 0.12$ m) generated by wave oscillatory flows.

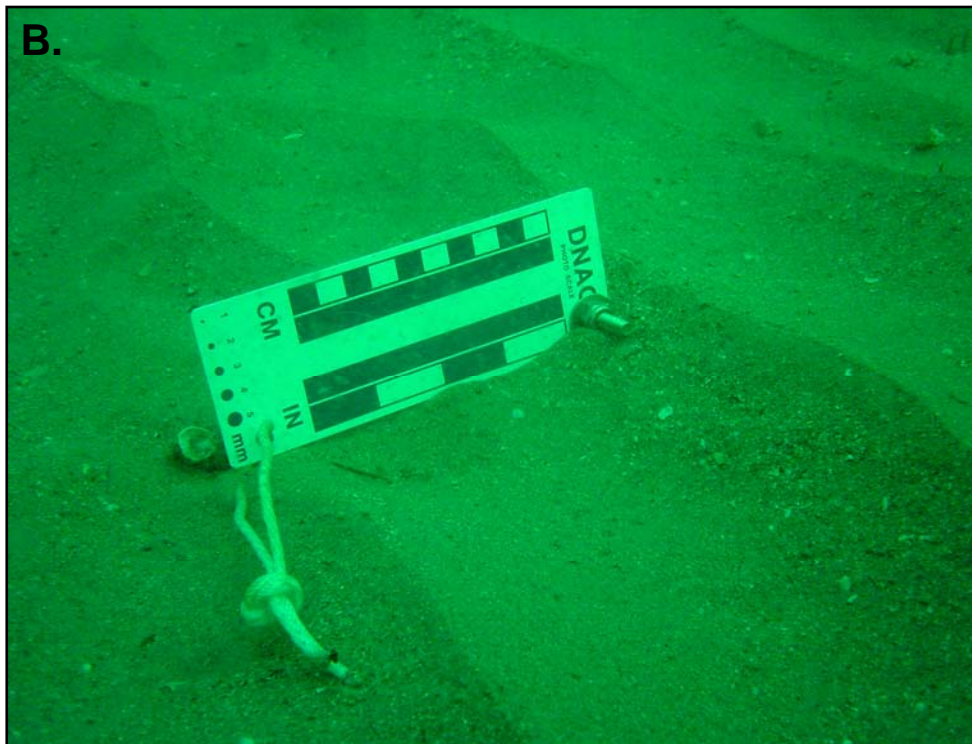


Fig. 8. Digital photographs of well-sorted fine sand sediment type located on lower sand flat. Ripple dimensions at the time of observation were $\lambda = 0.10 - 0.13$ m, $\eta = 0.05$ m.

Seasonal Averages of Hydrodynamic and Meteorological Data

For the purposes of this paper, seasons were defined to be consistent with the classic astronomical concept following the path of the earth along the ecliptic. Using this designation, June 21, the summer solstice, is assigned the first day of summer and December 21, the winter solstice, the first day of winter in the northern hemisphere. Spring thus begins on March 21, and fall on September 21, as these dates occur on the spring and autumnal equinoxes respectively. From April 2002 through October 2003, which is the extent of our hydrodynamic data covering the period of repeat sidescan sonar surveys, the average current magnitude 1.2 m above the seabed (mab) at the OB3 site was 5.8 cm s^{-1} and directed predominately from the south-southeast to the north-northwest across the inner-shelf. Mean current magnitudes varied little with season ranging from a low of 5.1 to a maximum of 6.4 cm s^{-1} . Maximum near-bottom current magnitudes were 26.1 cm s^{-1} and occurred during the offshore passage of Hurricane Isabel in September 2003. For all data collected, the mean current speed at 1.2 mab in the along-shelf direction was -0.20 cm s^{-1} from SW to NE and the mean across-shelf current speed was -1.9 cm s^{-1} in the onshore direction. For this study, positive along-shelf is defined as being directed from the northeast to the southwest and positive across-shelf is defined as being directed offshore. The maximum across-shelf speed for all deployments was -22.0 cm s^{-1} , which is directed onshore and maximum along-shelf speed was -23.8 cm s^{-1} , which is directed from southwest to northeast (Table 2).

The dominant wind direction during the nineteen-month period, as measured at Frying Pan Tower (FPT), was directed out of the southwest at 174 degrees and the average wind speed was 15.9 knots. The maximum recorded wind speed during this study was 62 knots and this occurred during the passage of Hurricane Isabel in September 2003. The average wave height at

Table 2. Seasonal near-bottom current flow data measured at 1.22 m above the bed (mab). Seasons are defined following the classic astronomical concept based on the earth's position along the ecliptic. *Data gaps occur during routine maintenance of instrumentation. All measurements are in cm s^{-1} . Positive along-shelf is directed to the southwest and positive across-shelf is directed offshore.

| | Summer 2002 6/21 - 9/20 | Fall 2002 9/21 - 12/20 | Winter 2002-03 12/21 - 3/20 | Spring 2003 3/21 - 6/20 | Summer 2003 6/21 - 9/20 | Fall 2003 9/21 - 12/20 | All Data 4/25/02 - 1/13/04* |
|---|----------------------------------|------------------------------|-----------------------------------|-------------------------------|-------------------------------|---------------------------------|-----------------------------------|
| Mean Current | 6.38 | 5.8 | 5.54 | 5.91 | 5.05 | 5.83 | 5.82 |
| Maximum Current | 19.1 | 19.8 | 19.5 | 25.6 | 26.1 | 23.3 | 26.1 |
| Mean Along-shelf velocity | -0.67 NE | 0.6 SW | -0.09 NE | -0.30 NE | 0.53 SW | -0.25 NE | -0.20 NE |
| Mean Across-shelf velocity | -1.39 onshore | -1.4 onshore | -2.34 onshore | -2.77 onshore | -1.62 onshore | -1.61 onshore | -1.91 onshore |
| Maximum Along- shelf velocity | -16.58 NE | -17.3 NE | -16.96 NE | -23.32 NE | -23.8 NE | 15.89 NE | -23.8 NE |
| Maximum Across-shelf velocity | -17.09 onshore | -19.1 onshore | -17.04 onshore | -21.54 onshore | -22.00 onshore | -21.22 onshore | -22.00 onshore |
| Maximum Semidiurnal Tidal Current | 4.90 | 3.4 | 3.77 | 4.42 | 3.37 | 3.63 | 4.90 |

the 5-mile study site, recorded by the ADCP, was 0.9 m and the average wave period was 7.3 seconds. The largest significant wave height on record was 2.6 m and occurred during the fall of 2003. Average seasonal near-bottom wave orbital velocities ranged from 7.9 cm s^{-1} to 11.4 cm s^{-1} with an overall study period mean of 9.8 cm s^{-1} . The maximum wave orbital velocity on record was 63.9 cm s^{-1} , again during the passage of Hurricane Isabel (Table 3).

Determination of Sediment Mobility

The Styles and Glenn (2002) bottom boundary layer model was used in this study to calculate bed shear stress and critical shear velocities due to both currents and the combined effects of waves and currents at the seabed. This model is an update of the 1987 Glenn and Grant continental shelf boundary layer model commonly used to determine flow and suspended sediment concentration profiles in the boundary layer overlying a non-cohesive, sand-dominated seabed. The new model version includes a stratification correction, which when field tested off the New Jersey coast, was demonstrated to be significantly better at predicting sediment transport, especially during storm events (Styles, 2000).

The model required the input of several parameters including time series data of the mean current (u_r) at a chosen reference elevation (Z_r) within the lower 1.2 mab, time series data of near-bottom wave orbital velocity (u_b) and wave excursion amplitude (A_b), both calculated using linear wave theory equations. Both the current time series data and wave data used to calculate wave orbital velocity were obtained from the ADCP at four hour intervals. The model also required the input of grain size distributions based on the surficial sediments prevalent at the study site as well as a default for ripple characteristics, and wave and current incidence angle. These input parameters were obtained through diver observations during standard instrument deployment and retrieval cruises at the OB3M site.

Table 3. Seasonal significant wave and acoustic backscatter signal (ABS) data obtained from the OB3M study site via an ADCP moored on the inner shelf (17.7 m depth). ABS signal is from the 1.22 m bin elevation above the seabed. For comparative purposes, data denoted in parentheses is from a mid-shelf (30 m depth) wave gauge approximately 64 km southeast of OB3M. H_s = significant wave height and u_b = near-bottom wave orbital velocity.

| | Summer 2002 6/21 - 9/20 | Fall 2002 9/21 - 12/20 | Winter 2002-03 12/21 - 3/20 | Spring 2003 3/21 - 6/20 | Summer 2003 6/21 - 9/20 | Fall 2003 9/21 - 12/20 | All Data 5/4/02 - 1/13/04 (5/1/02 - 1/31/04) |
|---|-------------------------------|------------------------------|-----------------------------------|-------------------------------|-------------------------------|------------------------------|--|
| Mean ABS (dB) | 58.81 | 60.46 | 60.29 | 59.86 | 60.39 | 60.68 | 59.89 |
| Maximum ABS (dB) | 68.89 | 78.9 | 70.54 | 69.71 | 72.6 | 71.78 | 78.9 |
| Mean H_s (m) | 0.9 (1.1) | 1.0 (1.3) | 1.0 (1.5) | 0.9 (1.3) | 0.9 (1.3) | 1.0 (1.5) | 0.9 (1.33) |
| Maximum H_s (m) | 2.1 (3.3) | 2.2 (4.5) | 2.1 (4.5) | 2.1 (3.5) | 2.5 (6.0) | 2.6 (5.1) | 2.59 (6.0) |
| Mean Period (sec) | 6.9 (7.3) | 7.2 (7.7) | 6.8 (7.5) | 6.9 (7.5) | 7.6 (8.0) | 7.5 (7.9) | 7.3 (7.6) |
| Maximum Period (sec) | 18.2 (16.7) | 16.0 (14.3) | 14.2 (14.3) | 12.8 (12.5) | 18.2 (20.0) | 18.2 (16.7) | 18.2 (20) |
| u_b Mean (cm s^{-1}) | 7.9 (10.4) | 10.0 (15.3) | 9.5 (16.5) | 8.8 (14.3) | 11.2 (18.6) | 11.4 (16.9) | 9.8 (14.9) |
| u_b Maximum (cm s^{-1}) | 37.5 (61.4) | 33.4 (77.2) | 42.9 (84.5) | 28.1 (59.4) | 63.9 (149.5) | 39.1 (94.3) | 63.9 (149.5) |

The model output provided time series data of bed stresses in response to near-bottom currents and the combined effects of waves and currents at the seabed. These data were computed for each season of the study period as well as for individual sediment mobility events hypothesized to be influential in mobilizing significant sediment amounts. Critical shear stress was calculated using the median grain size from surficial grab samples of fine sand bodies on the lower sand flat adjacent to the instrument site and critical shear velocity for the initiation of motion was provided in the model output. Similar to methods employed by Wren and Leonard (2004), a critical shear velocity for incipient suspension was calculated using the Rouse parameter (Middleton, 1984) for the median grain size within the fine sand bodies at the site (0.2041 mm) and was determined to be 2.46 cm s^{-1} . The required critical shear velocity for full suspension of sediment was also calculated using the Rouse parameter and determined to be 6.16 cm s^{-1} .

Tidal Currents

Harmonic analysis of the current time-series data collected 1.2 mab indicates that the dominant tidal frequency is the M2 semidiurnal constituent. This result agrees well with previous studies, which have shown that greater than 80% of the tidal energy present in the upper water column of Onslow Bay is controlled by the M2 tidal component (Pietrafesa et al., 1985). Tidal ellipse calculations at 1.2 mab yielded a major axis value of 3.1 cm s^{-1} and minor axis value of 0.37 cm s^{-1} . Orientation of the ellipse is 11.7 degrees north of east. A band-pass filter set at 10 - 16 h similar to Wright et al. (1999) was employed to separate semi-diurnal tidal currents in the near-bottom layer from remaining mean current flows. Near-bottom tidal currents at the 1.2 m elevation were consistently between 3.0 to 4.9 cm s^{-1} and showed little variability between neap and spring tidal cycles. To better constrain the potential effects of tidal currents on

sediment mobility periods of fair-weather (light winds and calm sea state) were identified and examined. This approach minimized the effects of other dominant physical forcing mechanisms, which may contribute to significant sediment mobility.

One such period was between July 2003 and September 2003 when a large area of high pressure dominated the region across Onslow Bay. Winds during this period averaged 13.2 knots and prevailed from the south, while average wave heights were generally below the long-term average of 0.9 m. During this period of fair-weather mean bottom tidal currents at 1.2 mab was 3.4 cm s^{-1} with a maximum of only 4.8 cm s^{-1} . Shear velocity due solely to currents (u_{*c}), assumed to be dominated by tides, did not exceed 0.25 cm s^{-1} . This is well below the calculated critical shear velocity of 1.33 cm s^{-1} needed to initiate movement of fine grain sediments typical of the study area.

Waves and Wind-driven Currents

Near-bottom wave orbital velocity was calculated using four hour wave height and period data obtained from the inner-shelf ADCP and applying standard linear wave theory equations. The average near-bottom wave orbital velocity for the entire study period was 9.8 cm s^{-1} with seasonal values ranging from 7.9 cm s^{-1} to 11.4 cm s^{-1} . Near-bottom wave orbital velocity was calculated using four hour wave height and period data obtained from the inner-shelf ADCP and applying standard linear wave theory equations. The maximum wave orbital velocity on record was 63.9 cm s^{-1} and occurred during Hurricane Isabel, which passed approximately 225 km offshore of the study area (Table 3).

The stress imparted to the seabed by wave-current interaction is several orders of magnitude greater than that of currents alone during a period of quiescent weather dominated by light winds and average to below average wave conditions. A simple correlation analysis

comparing the ABS signal at 1.2 mab (our proxy for suspended sediment within the water column) and near-bottom wave orbital velocity for all data collected, indicates a high degree of correlation ($r = 0.45$). Employing the critical threshold for initiation of sediment movement under the influence of waves and currents during the nineteen month period, it was calculated that the fine sand portion of the seabed was inactive less than 34% of the time.

The subtidal current contribution to the mean near-bottom current was obtained by applying a 33 h low-pass filter similar to Wright et al., (1999). Along-shelf and across-shelf subtidal current component flows were rotated parallel and perpendicular to the NE to SW trending coastline respectively, to aid in determining direction of transport during periods of elevated sediment mobility. The bulk of the low frequency signal is considered the product of surface winds and compares well with intensity and direction of local surface winds. Subtidal current direction, as well as the overall mean current at the 1.2 mab compared well with surface wind direction particularly in the along-shelf direction, and often responded rapidly to reversals in winds aligned in the along-shelf direction (Fig. 9). During this event, winds associated with an offshore area of low pressure remained directed out of the north-northeast at speeds above 15 knots for more than 72 hours before subsiding and switching to the south-southwest as the low pressure area departed to the north. The along-shelf component of the subtidal current responded accordingly and became directed to the southwest during this period. The weaker across-shelf subtidal component also responded to wind-driven flow reversals throughout the study; however, the relationship with wind direction and intensity was less developed.

Maximum subtidal current velocities ranging between 5.2 and 15.1 cm s^{-1} occurred during high-energy wind events (i.e. low pressure storm systems and frontal passages). The peak value measured for subtidal currents was 19.7 cm s^{-1} and was recorded during the passage of

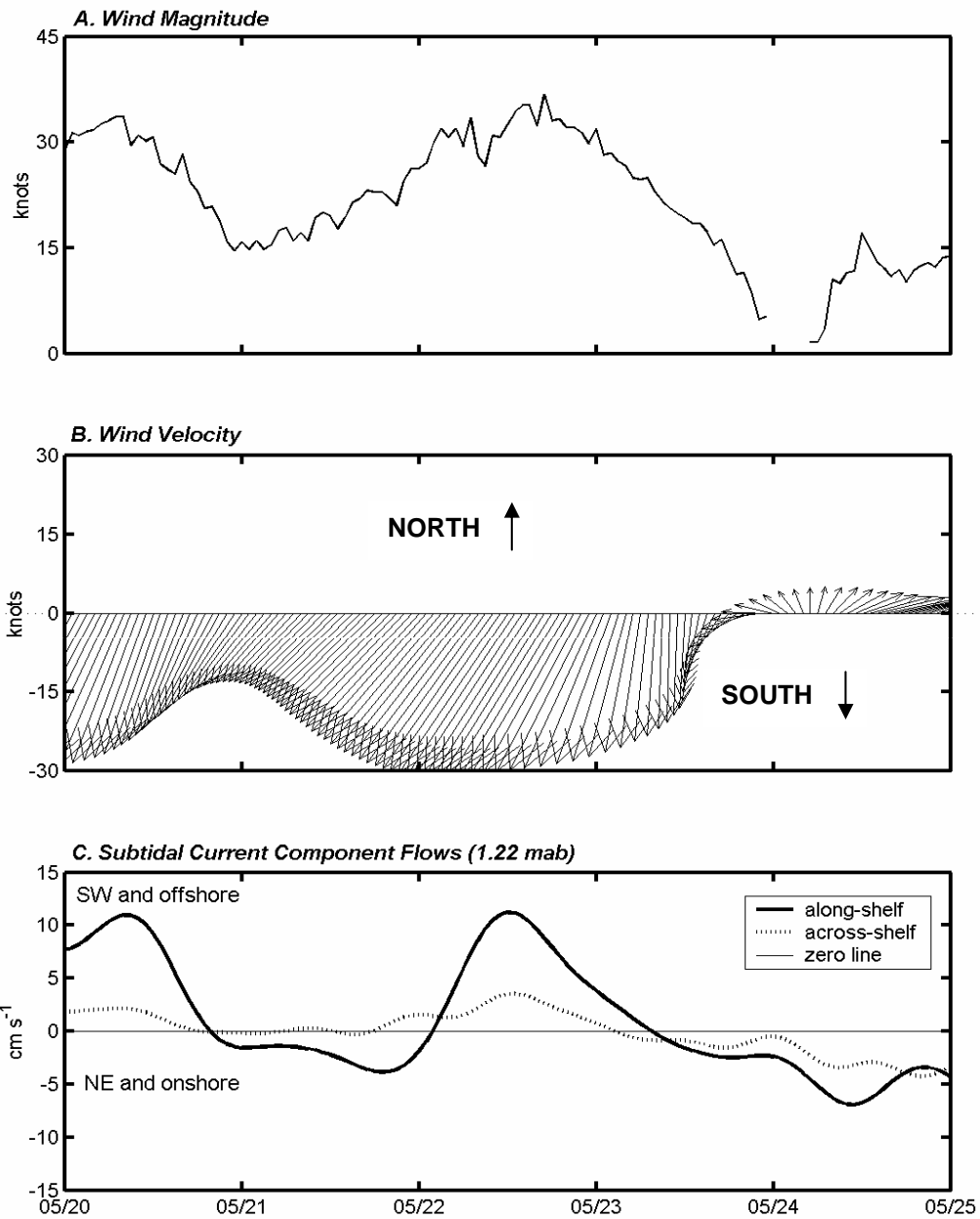


Fig. 9. Time-series of burst averaged parameters demonstrating subtidal current response at 1.22 mab from May 20 - 25, 2002, a significant event. (A, B) Wind speed and direction data obtained from Frying Pan Tower (FPT) C-Man station. (C) Subtidal along-shelf (solid) and across-shelf (dashed) component flows. Positive along-shelf is defined as being directed to the southwest and positive across-shelf is directed offshore. Dates are given in coordinated universal time (UTC) beginning at 0000 UTC.

Hurricane Isabel when winds remained elevated above 34 knots for more than 30 hours and exceeded 50 knots for more than 17 hours. Relative to the input by wave orbital velocities, subtidal currents were rather weak and rarely exceeded 10 cm s^{-1} . Wave orbital velocities, on the other hand, readily exceeded 20 cm s^{-1} for eighteen of the twenty three events. Factoring in waves and accounting for the synergistic effects of wave-current interaction, critical shear velocity due to waves and currents (u_{*cw}) exceeded critical thresholds for movement of the fine sand fraction of the seabed 66% of the time. Incipient suspended load was the primary means of mobility occurring 48.9% of the time, while movement solely as bedload took place 16.6% of the time. Full suspension of fine sand sediment was found to occur for less than 1% of the recorded period.

For all currents at 1.2 mab during the period of study, shear velocity due to solely to currents (u_{*c}) rarely exceeded critical values required for mobilization of fine sand found at the site. Bottom boundary layer model output indicated that only 53 instances of out of 3320 total data points surpassed the threshold for movement. This equates to less than 1.6% of the total study period. Further 15% of these sediment mobility events occurred during a sixteen day period in September 2003 when Tropical Storm Henri and Hurricane Isabel impacted the region and initiated strong subtidal flows.

High-energy Events Responsible for Sediment Mobility

Distinct sediment mobility events were identified using the acoustic backscatter signal (ABS) from the 1.2 elevation bin of the ADCP as a proxy for suspended sediment in the near-bottom zone. The criteria for identifying significant resuspension events was defined as those where the ABS signal exceeded 1.5 standard deviation of the average ABS at the 1.2 m elevation for a minimum of six consecutive hours. A total of twenty-three high-energy sediment mobility

events were identified (Appendix A). Current and wave data from the ADCP, and archived meteorological data from an offshore NOAA C-Man station (FPT) for the periods corresponding to these events, were then reviewed to determine the nature of the event.

Events were grouped into a broad classification system based on observed wind and atmospheric pressure data obtained from the Frying Pan Tower C-Man Station (Fig. 1), and through analysis of archived surface weather maps provided by the National Center for Environmental Prediction (NCEP). In this classification system, tropical systems were first delineated from extratropical events. These include tropical depressions, tropical storms, and hurricanes. Of the twenty-three events identified, four were tropical, with one becoming a major hurricane during the summer of 2003. The remaining nineteen events generated outside of the tropics were given the designation as extratropical due to genesis outside the tropics. These episodes were subclassed based on three general differentiating characteristics and anticipated sediment transport potential. The three classes were defined as, (1) defined areas of low pressure with at least one closed isobar affecting the region (strongest types labeled as nor'easters), (2) air mass frontal boundaries that generally approach from the west and south and may linger as stationary fronts for extended periods and are not associated with a local area of low pressure, and (3) fair-weather southerly wind events associated with high pressure conditions. All three classes were associated with above average sea-state, while the two former were also characterized by unsettled atmospheric conditions connected with storms. Depending on track and intensity, tropical events were associated with atmospheric conditions ranging from fair to windy and rainy, but always involve an elevated sea state, while southerly wind events tend to occur only under fair-weather. It is evident that different combinations of event type, intensity, track, and duration do occur and result in a dynamic range of atmospheric conditions. This

system of classification is by no means definitive and was constructed to help constrain the physical processes in the near-bottom zone resulting from atmospheric forcing.

The distinct sediment mobility vents spanned the nineteen-month period and occurred in higher frequency during the fall, winter, and spring months. Several were minor sediment mobility events. Thirty-nine percent narrowly met the six-hour criteria for mobilization lasting between six and twelve hours, while approximately 71% were sustained over periods of several hours to days. Seven events occurred in the spring, whereas fall and winter experienced six and five significant sediment mobility events, respectively, as outlined by study criteria. Only four events occurred in the summer months; however, three of the largest events on record took place during the last two weeks of the 2002 and 2003 summer seasons and all were tropical born.

Four sets of field data are presented below to illustrate near-bed response to changing surface conditions and to represent different levels of sediment mobility event intensity as well as the four major types of atmospheric conditions. These episodes are highlighted based on their predicted potential for mobilizing sediment and are as follows: (1) a late spring southerly wind event; (2) a fast moving nor'easter with associated cold front passage; (3) a slow moving, wind-dominated tropical storm event; and finally (4) a strong summer hurricane characterized by large ocean swells and high intensity winds (Table 4).

Southerly Wind Event: June 6 - 11, 2003

In the days leading up to this event, winds veered from the north to southeast direction following the passage of a moderate cold front across Onslow Bay waters. As the Bermuda high pressure expanded over offshore waters, its clockwise circulation produced moderate winds from the southerly direction for the 72 h period beginning at 0000 UTC on June 7. Winds ranged from less than 8 - 29 knots over this time. Wave heights at the inner-shelf study site rose slightly

Table 4. Summary of four major sediment mobility events observed between April 25, 2002 and October 14, 2003. Event 1) Subtropical Storm Gustav, 2) December extratropical low passage, 3) June southerly wind event, and 4) offshore passage of Hurricane Isabel. Currents are given at 1.2 mab.

| Event | Type | Winds (knots) | H _s (m) | T _p (sec) | u _b (cm s ⁻¹) | Mean current (cm s ⁻¹) | Subtidal current (cm s ⁻¹) | u* _c (cm s ⁻¹) | u* _{cw} (cm s ⁻¹) |
|------------------------|---------------------------|----------------|--------------------|----------------------|--------------------------------------|------------------------------------|--|---------------------------------------|--|
| 1. 6/7/03 - 6/10/03 | Southerly Wind Event (BH) | 10-30 SE-SW | 0.7 - 1.6 | 6 - 9 | 4.0 - 23.4 | 0.7 - 14.1 | 1.4 - 10.9 | 0.3 - 1.2 | 1.9 - 5.1 |
| 2. 12/25/03 - 12/27/03 | Extratropical Low (ETlo) | 10-50 SE-NW | 0.6 - 1.8 | 6 - 9 | 6.0 - 24.2 | 0.7 - 17.1 | 4.1 - 14.8 | 0.2 - 1.5 | 2.6 - 5.0 |
| 3. 9/8/03 - 9/13/03 | Tropical Storm (T) | 10-40 NE-NW-NE | 0.5 - 2.0 | 5 - 10 | 1.7 - 37.5 | 1.8 - 13.8 | 2.8 - 9.8 | 0.2 - 1.3 | 1.3 - 6.4 |
| 4. 9/15/03 - 9/20/03 | Hurricane (T) | 10-60 SE-N-SW | 1.0 - 2.5 | 5 - 18 | 1.2 - 63.9 | 0.2 - 26.1 | 1.9 - 19.7 | 0.2 - 2.1 | 1.1 - 8.6 |

during the initial wind shift to the south, from less than 1.0 m to greater than 1.5 m, at 0000 UTC on June 8 before slowly subsiding back to ambient fair-weather conditions by 1200 UTC on the 8th. A secondary peak occurred on June 9 in response to a slightly intensified wind field (Fig. 10C).

Mean current magnitude at 1.2 mab ranged from less than 1.0 to 14.7 cm s⁻¹ and was partially influenced by the semidiurnal tidal component input as demonstrated by the cyclic nature of the flow regime. As tidal currents moved in conjunction with the mean flow, currents increased in magnitude, and when they moved in the opposite direction the mean current was diminished. Overall, during the first 36 h of this event, the mean current flowed in the negative across-shelf direction and oscillated between the positive and negative along-shelf direction indicating a net motion in the onshore direction (Fig. 10A). The magnitude of subtidal flows displayed a consistent rise over the same period from 1.4 cm s⁻¹ to 10.9 cm s⁻¹ in response to sustained winds of approximately 20 knots out of the south and follows the direction of the mean component flows at the same depth (Fig. 10B). Waves approached from the south-southeast throughout the duration of the event and associated wave orbital velocities in the near-bed layer ranged from 4.0 to 23.4 cm s⁻¹ with more than 36 consecutive hours of the velocity exceeding 10.0 cm s⁻¹ between June 7 and June 9 (Fig. 10E).

During the 12 hour period bracketing 1200 UTC June 7 and 0000 UTC June 8, a sharp rise in the acoustic backscatter signal at the 1.2 mab occurred (Fig. 10G), and remained elevated for the remainder of the sediment mobility event. It is fair to say that in conjunction with moderate, slowly varying winds from the southerly direction and above average wave orbital velocities, that sediment was indeed being mobilized during this high-energy, yet fair-weather period. Calculated shear velocities due to the synergistic effects of waves and currents (u_{*cw})

also favored sediment mobilization during this time. For a 72 h period, u_{*cw} values remained above 1.33 cm s^{-1} insuring, at the very least, that the fine-grained sand fraction of surficial seabed material would be mobilized as bedload. Further, the combined wave-current shear velocity exceeded the 2.46 cm s^{-1} value needed for incipient suspension for 60 of the 72 hours defined in this event (Fig. 10F). Together this evidence suggests a moderate sediment mobilization event even though high pressure and fair-weather conditions dominated the inner-shelf surface waters.

In terms of transport for this event, subtidal flows driven by the slowly varying surface wind pattern became directed in the negative across-shelf direction during the period of maximum conditions, at the same time, waves approaching the coast from south-southeast caused fine sand bedload migration to the north in the along-shelf and onshore. Once incipient suspended load conditions were exceeded, the weak (7 to 10 cm s^{-1}) subtidal flows had greater potential to transport the episodically suspended materials in the onshore direction in combination with contributions from wave oscillatory motions. This scenario favors transport of significant amounts of previously mobilized sediment both onshore and to the north in response to the combined effects of subtidal currents and waves (Fig. 10).

Extratropical Low and Frontal Passage: December 23 - 28, 2002

On December 24, 2002 an extratropical cyclone and trailing cold front approached the coastal waters of southeastern North Carolina from the west. Ahead of the cold front, south-southwest winds increased in intensity from approximately 7 knots at 0900 UTC December 25 to more than 45 knots by 1600 UTC and remained elevated above 30 knots from the southwest through 0400 UTC on December 26. At this point, the cold front passed offshore of the FPT NOAA C-Man Station and winds abruptly veered to the west-northwest while remaining sustained above 20 knots for 12 successive hours from this new direction. Wave

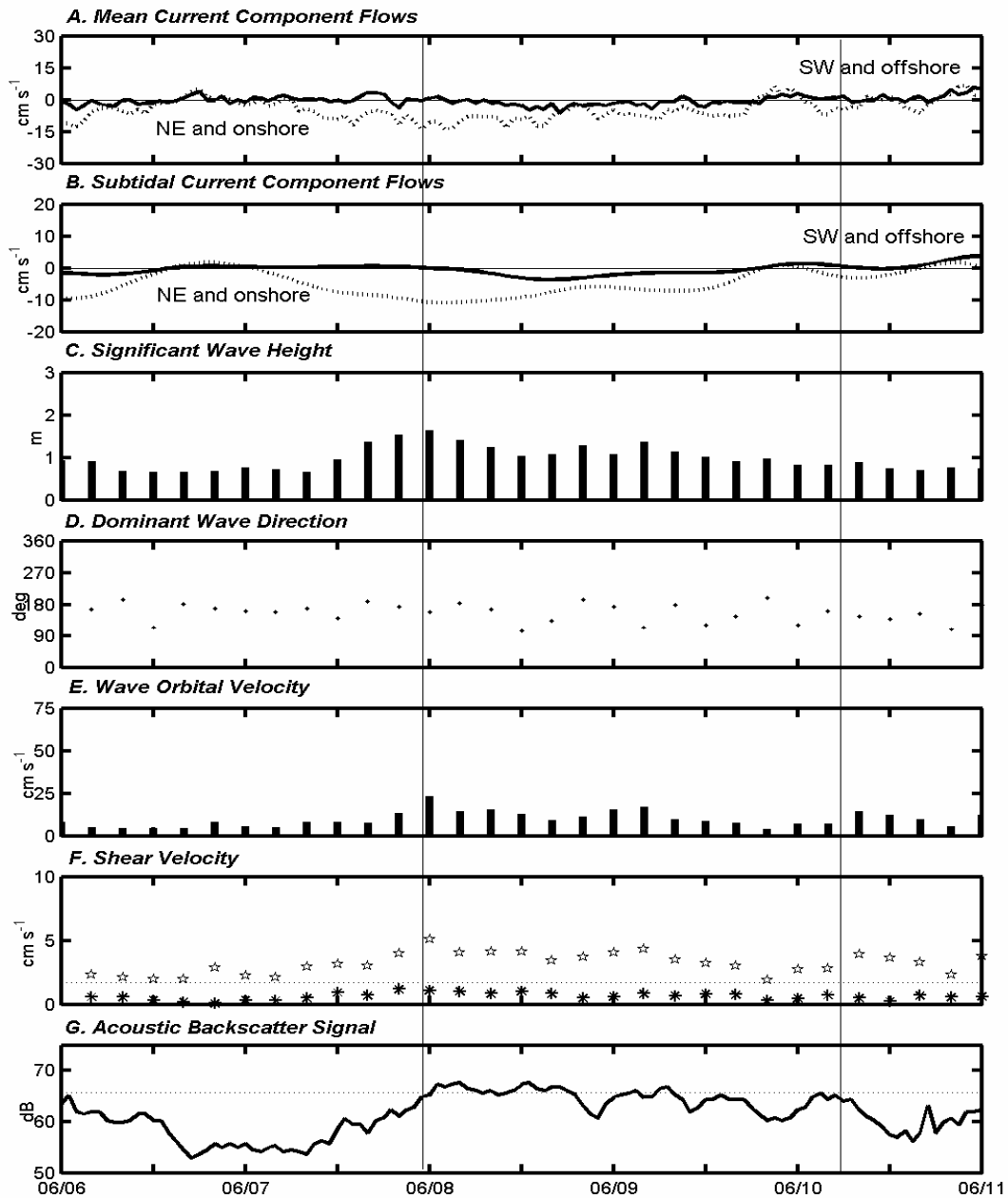


Fig. 10. Southerly wind event sediment mobility evidence. (A) mean along (solid) and across-shelf (dashed) current at 1.22 mab, (B) subtidal along (solid) and across-shelf (dashed) current at 1.22 mab, (C) significant wave height, (D) dominant wave direction, (E) near-bottom wave orbital velocity, (F) shear velocity due to currents (asterisk) and shear velocity due to waves and currents (star), and (G) acoustic backscatter signal at 1.2 mab. Positive along-shelf is defined as being directed to the southwest and positive across-shelf is directed offshore. Dates given are in coordinated universal time (UTC) beginning at 0000 UTC. Paired vertical lines outline duration of event.

heights during this period, ranged from 1.0 to 1.75 m through 1800 UTC on December 25, and slowly subsided to below 1.0 m as winds turned to the west-northwest after passage of the cold front. Wave direction maintained a south-southeast approach and wave period remained consistent between 6 - 9 seconds throughout the entire 48 period of interest (Figs. 11C, D).

Mean currents were initially quite weak remaining less than 10 cm s^{-1} for the first 25 hours as surface winds steadily increased in velocity from the south-southwest. By 0000 UTC on December 26 mean current magnitude topped 10 cm s^{-1} and averaged 13.2 cm s^{-1} for the next 17 hours, even as surface winds subsided to ambient conditions. Subtidal current magnitude followed suit ranging from 10 to 15 cm s^{-1} during the same period. Although missing a portion of data for the period, the trend in wave orbital velocity follows that of the maximum winds and ranges from 9.9 to 24.2 cm s^{-1} from 1200 UTC on December 25 through 1600 UTC on December 26. Following this peak in wave orbital velocity, a peak in acoustic backscatter signal in the near-bottom layer followed several hours later and exceeded criteria levels for eleven successive hours indicating sediment suspension during this period through at least the lowest 1.2 m of the water column (Fig. 11E, G). Further, shear velocity, u_{*cw} , exceeded the critical value for fine sands thereby enabling incipient suspension for the entire forty eight hour event, nonetheless shear velocities never reached levels permitting full suspension of fine grain sand bottom sediments (Fig. 11F).

Subtidal currents responded to the changing surface wind regime, which potentially affected the transport path of mobilized sediment that had become suspended (Fig. 11B). As indicated by the shear velocity calculation, bottom sediments contained in the fine sand bodies would have been, at the very least, mobilized as transitional bedload throughout the entire event. Initially, fine-grained sands momentarily suspended would be directed along-shelf in the

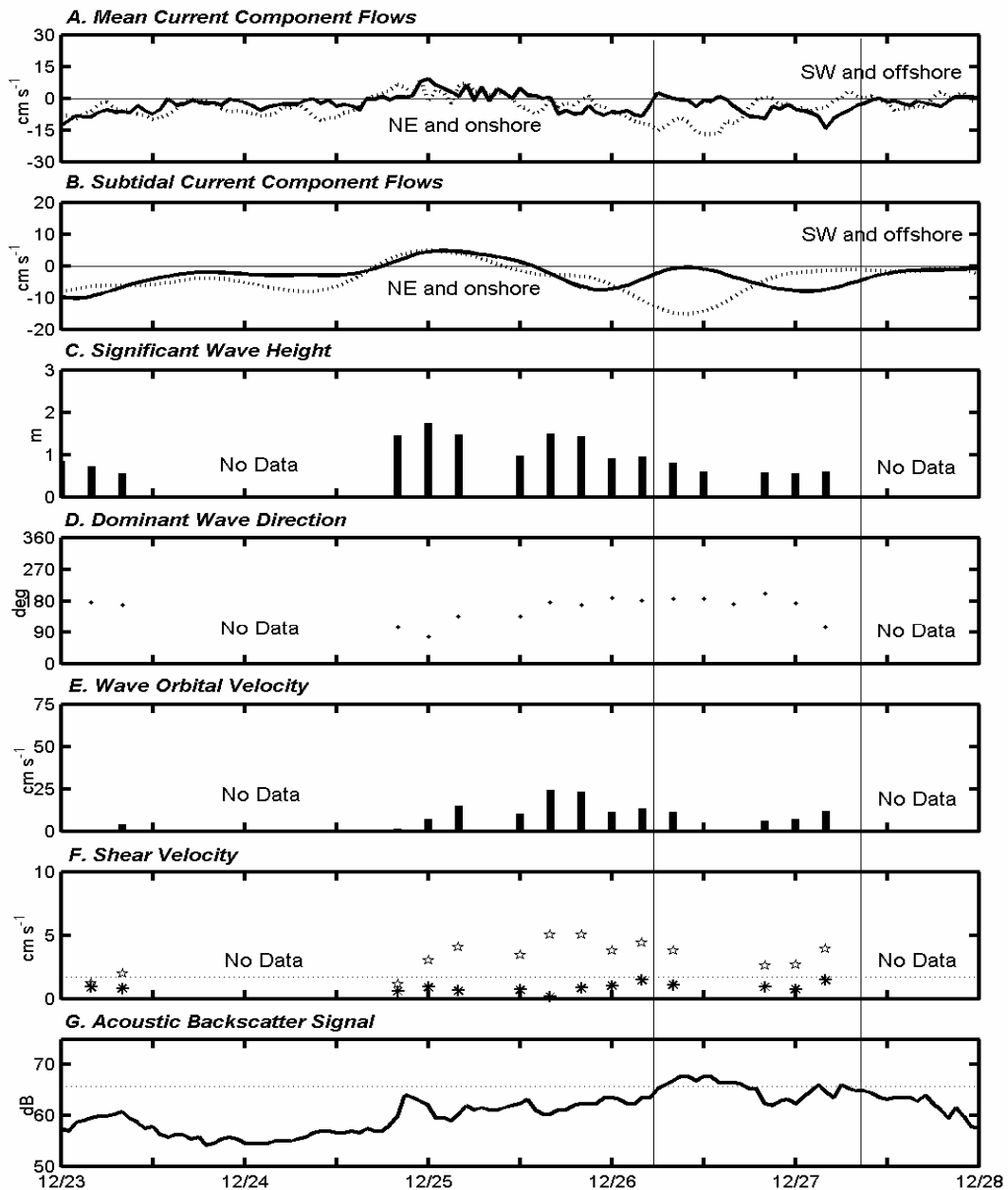


Fig. 11. Evidence for sediment mobility from December 25, 2002 extratropical low. (A) mean along (solid) and across-shelf (dashed) current at 1.22 mab, (B) subtidal along (solid) and across-shelf (dashed) current at 1.22 mab, (C) significant wave height, (D) dominant wave direction, (E) near-bottom wave orbital velocity, (F) shear velocity due to currents (asterisk) and shear velocity due to waves and currents (star), and (G) acoustic backscatter signal at 1.2 mab. Positive along-shelf is defined as being directed to the southwest and positive across-shelf is directed offshore. Dates given are in coordinated universal time (UTC) beginning at 0000 UTC. Paired vertical lines outline duration of event.

southwest to northeast direction with very little onshore or offshore movement. This would have occurred prior to the frontal passage when winds were directed from the south and southwest. After the wind switch to the NW, and coincident with the period of highest ABS signal at 0800 UTC, the subtidal current component abruptly increased to more than 15 cm s^{-1} in the negative, which would favor driving suspended sediments in the onshore direction. The along-shelf component remains negligible ranging from 0 to -5 cm s^{-1} , which would direct currents to the southwest. More importantly, the across-shelf component rapidly increases to more than 15 cm s^{-1} in the negative, which would favor driving suspended sediments in the onshore direction. Simultaneously, sediment is still in part being moved to the north as bedload by waves approaching from the south (Fig. 11D). Again, this scenario suggests that the primary direction of transport under the maximum conditions of this event was in the onshore direction in the across-shelf and to the north-northeast in the along-shelf.

Tropical Storm Gustav: September 7 - 12, 2002

Tropical storm Gustav developed approximately 725 km south-southeast of Cape Hatteras under a deep upper level trough on September 8, 2002. Gustav was unique in that it originated as a subtropical storm, but later developed tropical characteristics. Further, the duration of Gustav was much longer than most tropical systems, which normally move rapidly through the region. This system moved slowly to the north and northeast off the North Carolina coast for more than two days. Accordingly, it is considered representative of both a moderate nor'easter type storm and moderate intensity tropical system, both being common high-energy events that frequent the southeast U.S. coast in late summer and early fall seasons.

Beginning at 0000 UTC on September 9, winds at the NOAA Frying Pan Tower (FPT) C-Man station began to increase steadily from 20 knots to more than 30 knots from the east-

northeast direction indicating the advance of Tropical Storm Gustav. Simultaneously, increasingly higher period waves ($T_p = 8-10$ s) began approaching from the same direction (Fig. 12C). Winds reached a peak velocity of just over 40 knots from the north early on September 10 and then slowly veered to the west-northwest and subsided to less than 20 knots by 1200 UTC on September 11 as Gustav began to move quickly off to the northeast. Wave heights remained between 1.6 and 2.0 m during the twenty-four hour period between 1200 UTC September 9 and 1200 UTC September 10 and quickly subsided after this point (Fig. 12D).

Mean currents in the near-bottom ranged from 1.8 to 13.8 cm s^{-1} , reaching a maximum at 1200 UTC on September 11. These currents were initially dominated by the semidiurnal tidal component as evidenced by the well-defined periodicity in both the along- and across-shelf component (Fig. 12A). As winds increased in intensity from the east-northeast on September 9, the mean current flow responded and became directed to the southwest. This response is also evident in the subtidal flow regime, which here is assumed to be a direct product of the surface wind field. Subtidal flows during this event reached a maximum of only 9.8 cm sec^{-1} . The along-shelf component flow was directed to the southwest at less than 10 cm s^{-1} for the duration of the event. The flow quickly changed to the northeast direction early on September 11 as the winds switched from the northerly direction to the southwest direction (Fig. 12B). The across-shelf subtidal component remained very weak throughout the event and did not exceed 5 cm sec^{-1} .

A coincident peak in wave orbital velocity and ABS signal occurred between 1300 UTC on September 9 and 2300 UTC on September 10. For the next 34 h, ABS remained above criteria levels and wave orbital velocity increased from ambient levels ($< 10 \text{ cm s}^{-1}$) to more than 37 cm

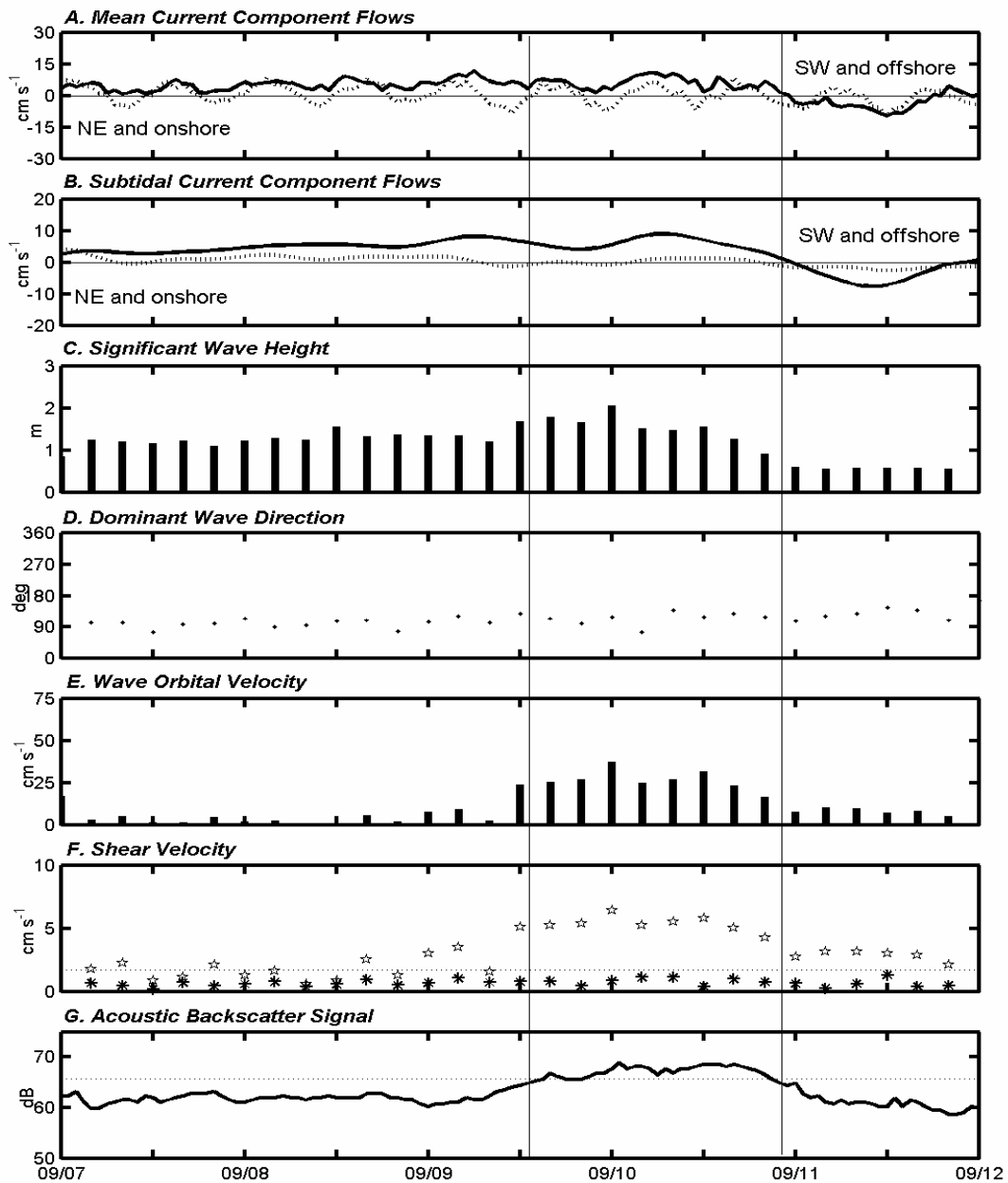


Fig. 12. Tropical Storm Gustav sediment mobilization evidence. (A) mean along (solid) and across-shelf (dashed) current at 1.22 mab, (B) subtidal along (solid) and across-shelf (dashed) current at 1.22 mab, (C) significant wave height, (D) dominant wave direction, (E) near-bottom wave orbital velocity, (F) shear velocity due to currents (asterisk) and shear velocity due to waves and currents (star), and (G) acoustic backscatter signal at 1.2 mab. Positive along-shelf is defined as being directed to the southwest and positive across-shelf is directed offshore. Dates given are in coordinated universal time (UTC) beginning at 0000 UTC. Paired vertical lines outline duration of event.

s^{-1} (Fig. 12E, G). As Gustav moved further northward on September 11, wave heights and wave orbital velocities subsided due decreasing wind intensity and a shift in wind direction from onshore to offshore.

Combined wave-current (u_{*cw}) shear velocities ranged from more than 2.0 to 6.4 cm s^{-1} for approximately 36 h coinciding with the peak in ABS signal (Fig. 12F). When compared to the calculated Rouse numbers for the fine-grained sands that dominate this locale, incipient suspension would have been ongoing over this period. In addition, a very brief period (<8 h) of full suspension occurred between 2000 UTC on September 9 and 0400 UTC September 10. Thus, a significant portion of the fine-grained fraction of the bed surface was at least suspended periodically and sediment mobilization during the event was most likely significant.

During peak conditions, it is likely the fine sands on the seabed were being driven in the easterly direction as bedload under the influence of wave driven oscillatory flows (Fig. 12D). As indicated by shear velocity values for the same period, much of this sediment (< 0.2041 mm) was also being temporarily entrained into the water column as incipient suspended load. Once off the bottom, the motion of this material was governed primarily by the dominant current in the near-bed layer, which during peak conditions was a wind-driven along-shelf subtidal flow directed from northeast to southwest at magnitudes ranging from 0 to 9.8 cm s^{-1} . The across-shelf subtidal flow at this time remained negligible (Fig. 12B). Although weak, these currents are capable of transporting sediment suspended in the near-bottom short distances to the southwest over the 36 h period of maximum mobilization. Acting in concert, waves and subtidal currents then potentially set up a net transport of fine-grained sediment to the southwest in the along-shelf direction and onshore in the across-shelf direction.

Hurricane Isabel: September 15 - 20, 2003

Hurricane Isabel developed off the west coast of central Africa and was named on September 6, 2003. It continued a northwestward track for the next several days intensifying to a strong Category 5 hurricane on the Saffir-Simpson Scale early on September 12 and began impacting the coastal waters of Onslow Bay on September 15. By September 17 winds reached tropical storm strength (> 34 knots) and remained above this threshold for more than 30 hours. From 1600 UTM September 17 to 0500 UTM September 18 (14 h), winds were strong out of the N-NE. After passage of the central hurricane eye approximately 225 km east of Onslow Bay on September 18, winds quickly backed to the W-SW for more than 15 h. The highest winds recorded (>60 knots) occurred during this period.

Isabel was the largest magnitude event recorded during the period of study and began to impact the shelf waters offshore of Wrightsville Beach early on September 15 when long period swells ($T_p > 18$ s) began to approach from the southeast. Significant wave heights through the event remained elevated above the average of 0.9 m and reached a maximum of 2.5 m (Fig. 13C). Throughout the duration of the event near-bottom wave orbital velocities associated with the long period swells mobilized fine-grained sands at the OB3M study site. Later, increasingly high-velocity winds generated a localized short-period wave field atop the long period swell, which also contributed to mobilization of surficial bottom sediments.

Between September 15 and September 16, the near-bottom mean current attained velocities between 0.2 and 10 cm s^{-1} at 1.2 mab. These currents were highly variable in direction prior to September 17 due to the dominance of the M2 semidiurnal tidal component. During storm maximum, however, mean currents reached 26.1 cm s^{-1} , the highest on record during the entire study period. Subtidal currents ranged from 1.9 to 19.7 cm s^{-1} during the time, but

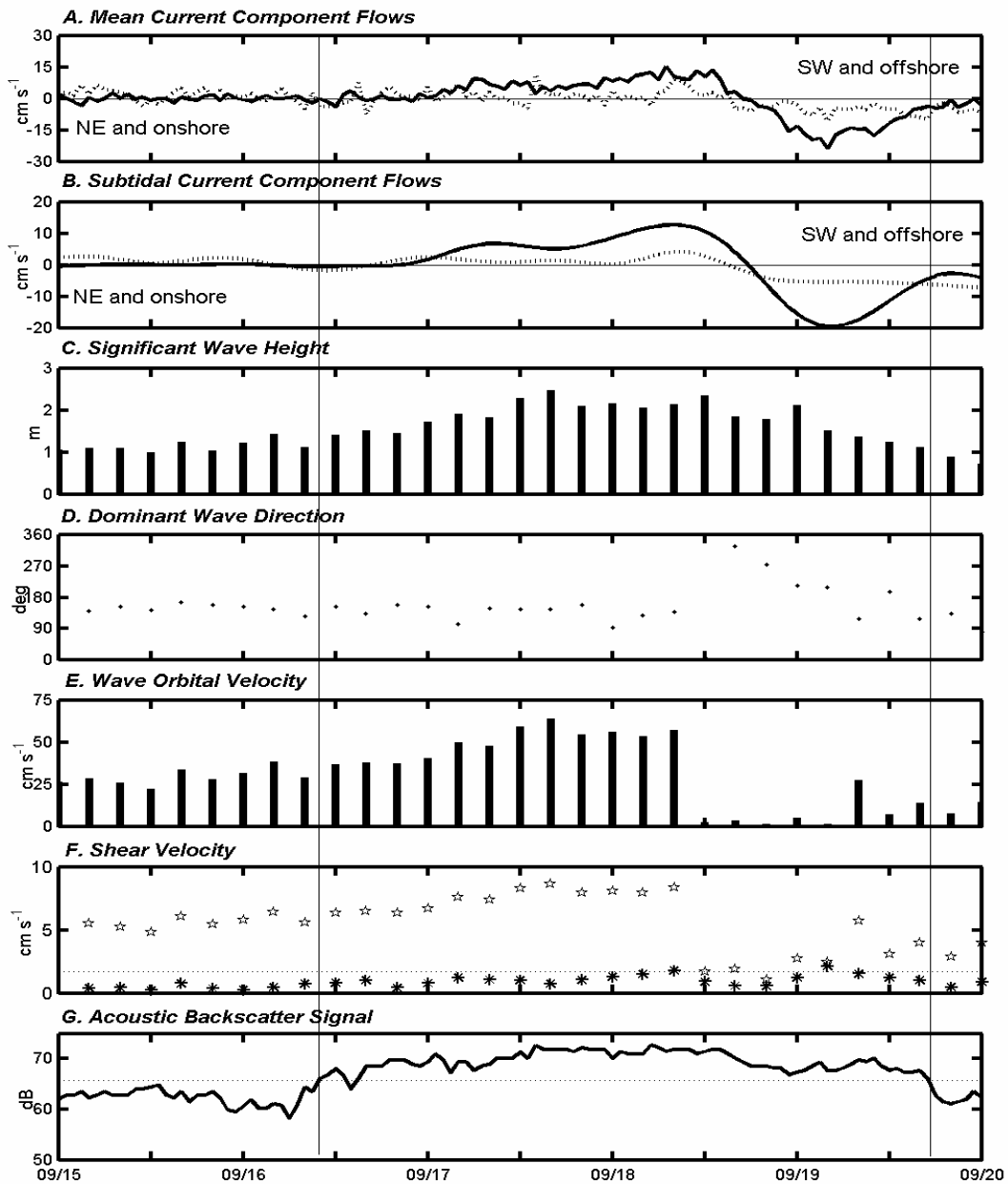


Fig. 13. Hurricane Isabel sediment mobility evidence. (A) mean along (solid) and across-shelf (dashed) current at 1.22 mab, (B) subtidal along (solid) and across-shelf (dashed) current at 1.22 mab, (C) significant wave height, (D) dominant wave direction, (E) near-bottom wave orbital velocity, (F) shear velocity due to currents (asterisk) and shear velocity due to waves and currents (star) and (G) acoustic backscatter signal at 1.2 mab. Positive along-shelf is defined as being directed to the southwest and positive across-shelf is directed offshore. Dates given are in coordinated universal time (UTC) beginning at 0000 UTC. Paired vertical lines outline duration of event.

increased in intensity due to forcing by the local wind field as Isabel approached and then passed east of Onslow Bay waters. Wave orbital velocities ranged from 20 cm s^{-1} to greater than 40 cm s^{-1} during storm approach, but during storm maximum ranged between 40 and 63 cm s^{-1} (Fig. 13E). Calculated shear velocity values indicate that under these conditions, fine sands would become fully entrained as suspended load and coarse sand material would begin to be agitated under the stresses imparted by wave action. This is further evidenced in sidescan sonar data collected post-storm that demonstrates a “freshening” of symmetrical wavelength megaripples within coarse sand bodies as well as minor changes in the orientation of these bedforms. Very coarse sand to sandy gravel-sized bedforms at similar depths ($<30 \text{ m}$) are believed to be only reactivated during extreme conditions (Riggs et al., 1996; Thielert et al., 2001) such as those associated with peak conditions during Isabel. This study shows that it is only during these very extreme high-energy events are critical shear velocities reached to allow the mobilization of the coarse grain sediments.

Combined wave-current shear velocity ranged from 1.7 to 8.6 cm s^{-1} for 72 successive hours with maximum shear velocities coincident with the period of maximum wave activity (Fig. 13F). Again employing the Rouse Parameter, these conditions easily exceed critical values required to mobilize fine sands present on the inner-shelf seabed. Further, shear velocities in excess of 6.2 cm s^{-1} would produce full suspension of fine grain sands (diameter $\leq 0.2041 \text{ mm}$). These conditions were met for 36 consecutive hours between 0000 UTC on September 17 through 1200 UTC on September 18. An elevated ABS obtained during the period and fine-grained sand collected in a sediment tube mounted 0.23 m above the bottom further indicate the suspension of bottom sediments (Fig. 13G).

Prior to full suspension, fine sands were found to be mobile as bedload and as incipiently suspended load. During this time, the direction of transport is believed to be dominated primarily by wave orbital velocity and the direction of wave approach. Dominant wave direction was from the east-southeast, which would create a net transport to north in the along-shelf and onshore in across-shelf direction period (Fig. 13F). The fraction of fine sand material temporarily suspended above the bed would again be influenced by the prevailing current direction, which in this case was from northeast to southwest in the along-shelf.

Once in suspension these sediments are likely to have been transported by means of the above average subtidal currents, produced via high velocity winds at the surface, which increased over this time from less than 5.0 cm s^{-1} to greater than 19.5 cm s^{-1} . These flows initially directed in the positive along-shelf direction and negligibly in the cross-shelf direction favored transport of suspended sediment predominately southwestward. After the wind switch to the west-southwest direction, the subtidal currents responded and became directed in both the negative along-shelf and across-shelf directions, which supports transport of sediment remaining in the water column to the northeast and onshore directions (Fig. 13B).

Sidescan Sonar Change Detection Analysis

Six areas on the lower sand flat adjacent to the marine hardbottom reef at the OB3M site were chosen to perform a change detection analysis across the time series of mosaics (Fig. 14). The objective of the change detection analysis was to determine trends in mobility of both the fine and coarse grain sand bodies and to attempt to link this mobility (or lack there of) to near-bottom layer hydrodynamic conditions produced in response to significant seasonal meteorological events. Areas were selected based on distinct high/low backscatter signatures that created highly visible, well-defined contact zones between adjacent lithofacies of surficial

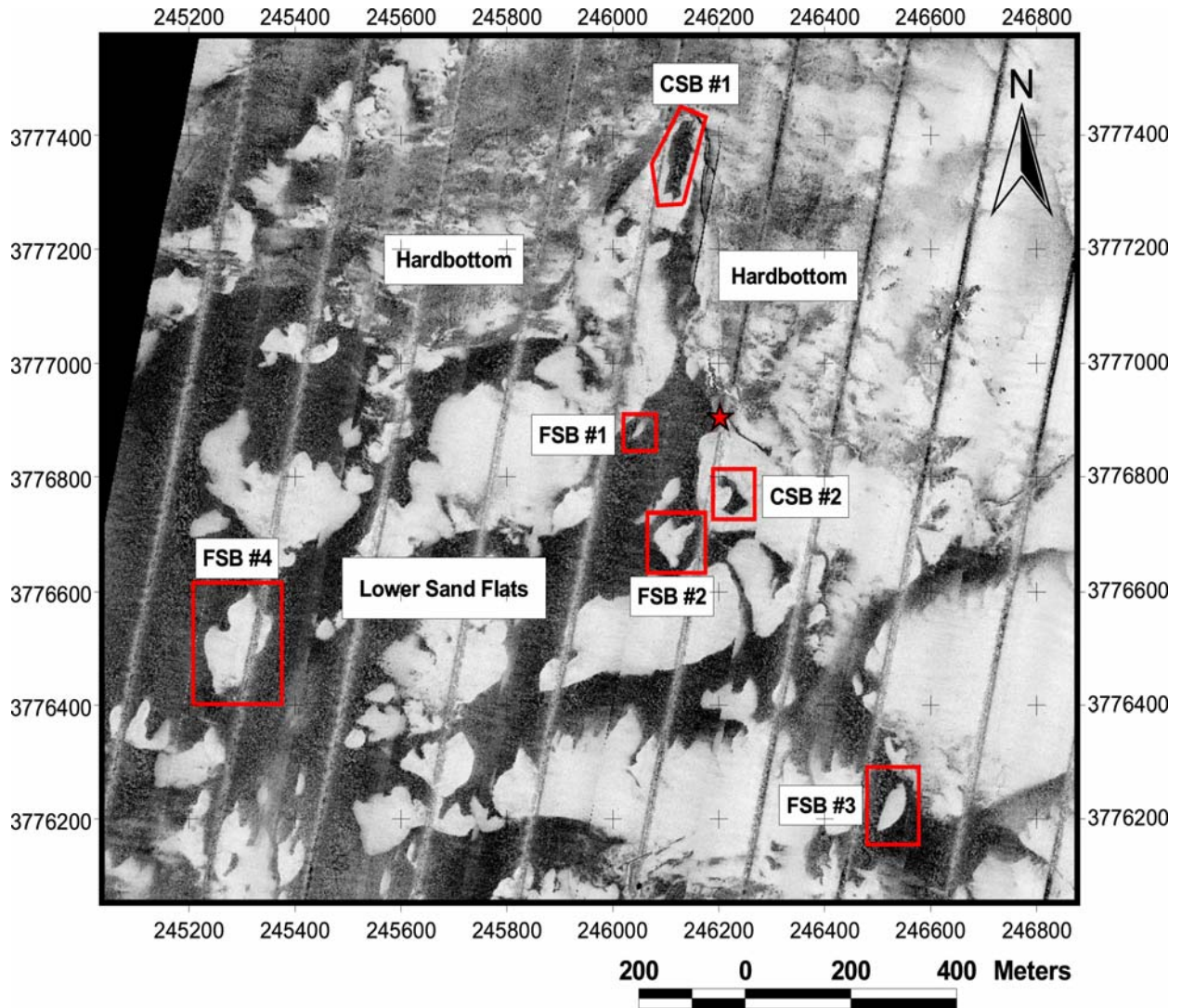


Fig. 14. Location of 6 subareas where change detection analysis was performed using biannual sidescan (100 kHz) surveys. Subareas were chosen based on proximity to both the marine hardbottom area and to CORMP ADCP instrumentation (denoted by star). Mosaic image was obtained March 14, 2002

sediment cover. Two subareas, consisting primarily of gravelly coarse sands (CS#), and four subareas of the presumably more mobile fine sand fraction (FS#) were chosen (Fig. 14).

Due to the inherent error that accompanies DGPS measurements during sonar acquisition and the subjectivity in the digitizing process of the fine/coarse sand contacts, a 10 m error tolerance buffer was introduced around the perimeter of each selected subarea (Fig. 15). Displacements beyond this buffer were considered significant. The 10 m buffer is likely to be a conservative estimate of the potential error introduced as the marine hardbottom as well as two sunken barges (Fig. 3) provided a natural, nonmoveable set of benchmarks on which the individual sonar lines from repeat surveys were aligned. Thus, subareas selected closer to these regions were better resolved in space and were more likely to be accurately geo-referenced, thereby limiting the error introduced via DGPS measurements. Subareas were typically chosen toward the center of the swath, but offset from the nadir region, to avoid pixel distortion introduced with increased grazing angle of the sonar beam toward the edges of the line. An example of the overlays used to perform change detection analysis is given in Fig. 16 and specific steps for performing change detection analysis using this methodology can be found in Appendix C. Expanded results for each subarea are also given in Appendix D.

Coarse Sand Body One (CSB-1)

The CSB-1 area is located within a sheltered portion of the lower sand flat where the 1.5 meter high crescent-shaped hardbottom reef bounds much of the sand body perimeter at distances ranging from 3 to 80 m. The northern boundary of the body is most sheltered (3 to 14 m from reef ledge), yet exhibited a moderate degree of morphological change varying as much as +/- 7 m in variable direction between the four surveys (Table 17A). The western contact was highly stable survey to survey wavering only +/-4 m in an inconsistent direction along its entire

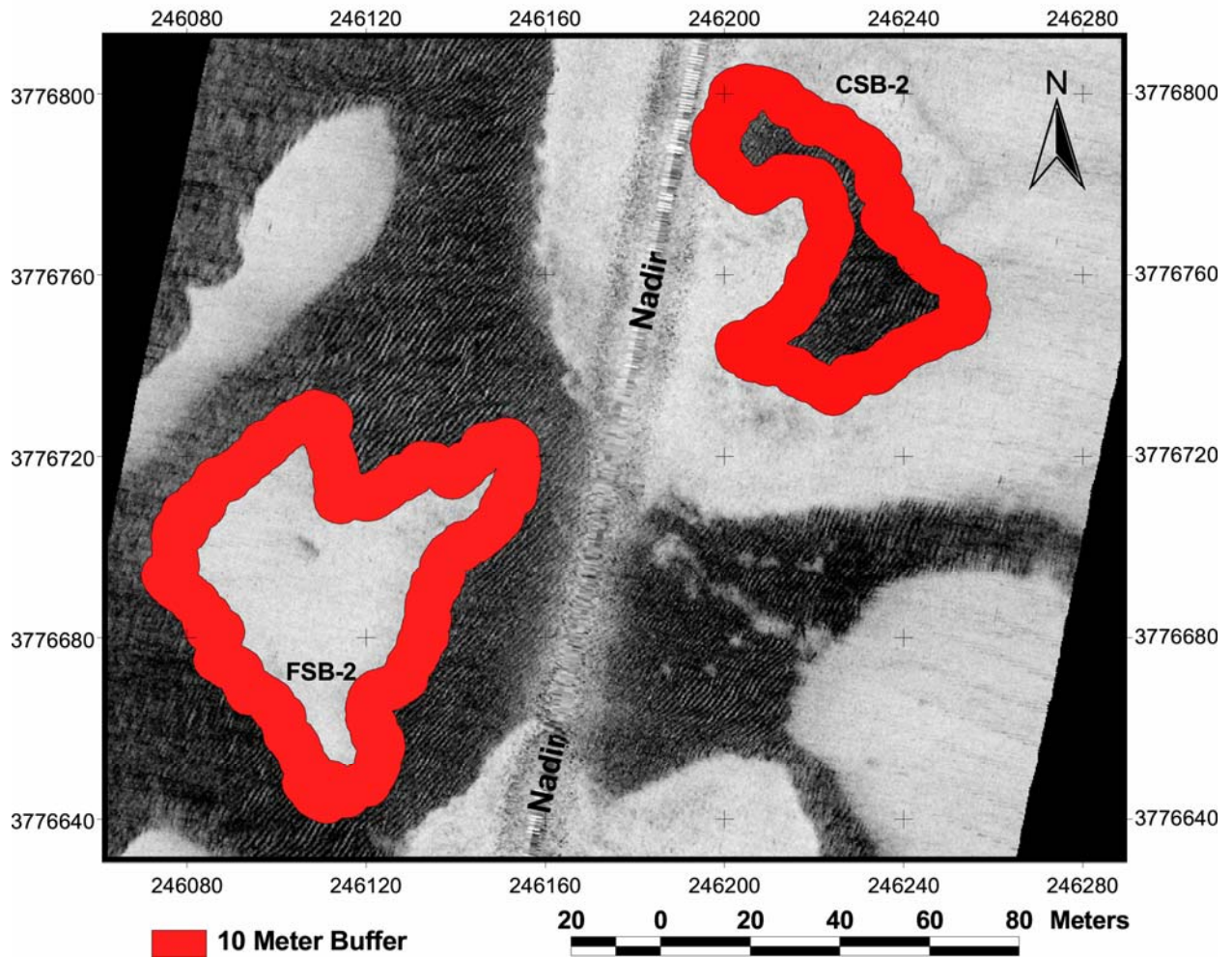


Fig. 15. Ten meter error buffer surrounding subarea sand bodies located on the lower sand flat where change detection analysis was performed.

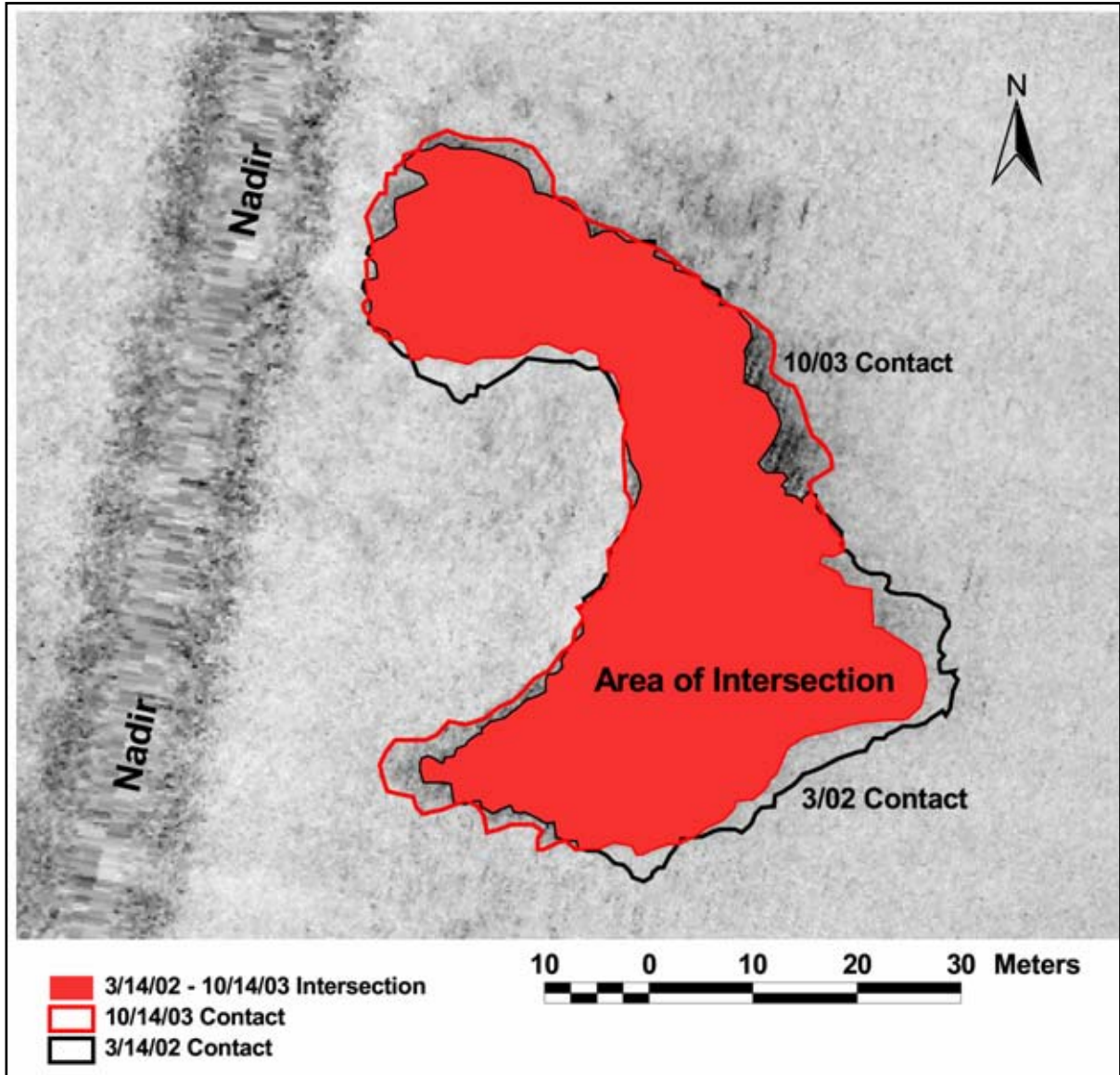


Fig. 16. Sand contact displacement results from CSB-2 spanning the period between March 2002 and October 2003.

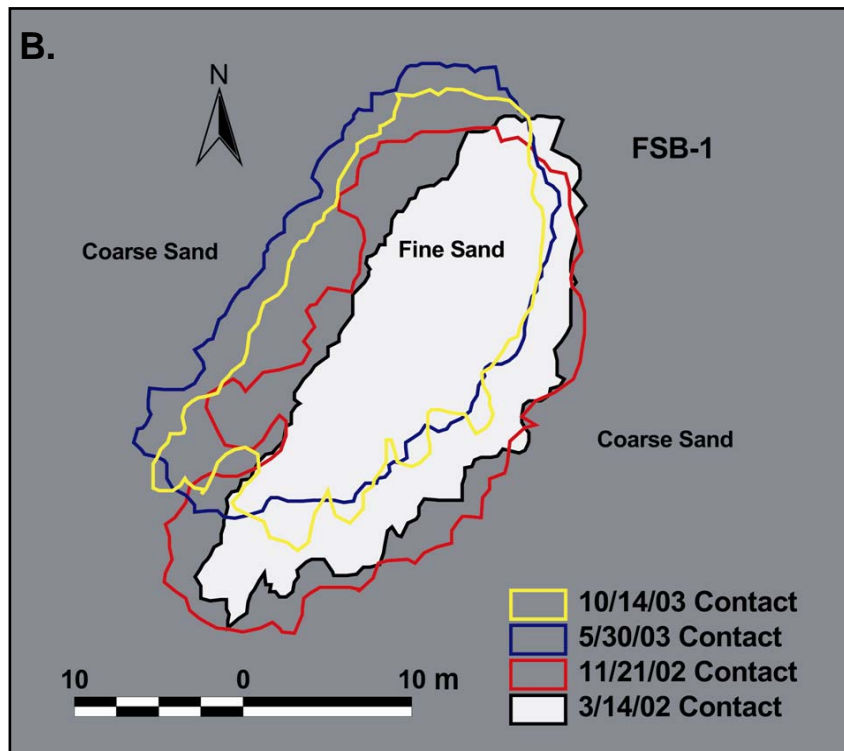
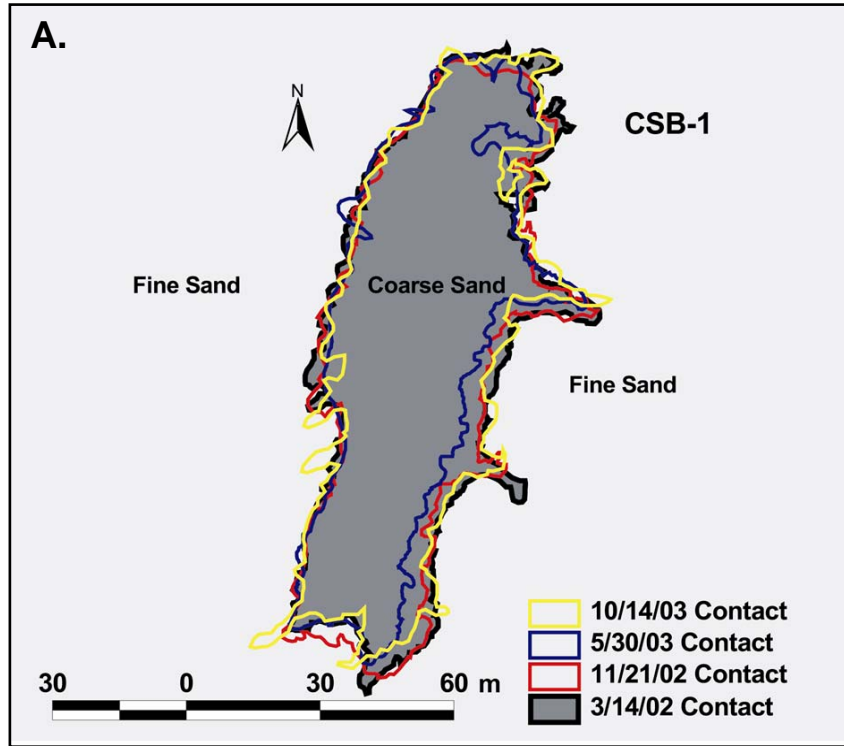


Fig. 17. CSB-1 and FSB-1 sand body contacts.

flank, while the eastern edge migrated westward between the fall 2002 and spring 2003 surveys, before shifting eastward again at the fall 2003 survey date to a position very similar to that of the fall 2002 survey. The displacement of these contacts at no point exceeded the 10 meter error tolerance buffer and there was no identifiable net displacement of the body during the course of the four surveys conducted (Table 5). Areal extent, however, of the sand body itself was deemed significant. It reached a minimum of 3870 m² in spring of 2003 and experienced a maximum of 4775 m² during the initial survey of spring 2002, for a change of nearly 1000 m² over the fourteen-month period. Also of note are the emergence, deletion, and migration of randomly placed fingers of coarse sediment along the boundary edge from survey to survey. These fingers seem to be a result of fine sands bordering the coarse sand body becoming mobilized and in the process covering and uncovering the less mobile coarse sand fraction. Given the proximity of CSB-1 to the location of the fixed hardbottom ledge, these data are regarded to be highly reliable, such that the 10 m buffer is considered overly conservative.

Fine Sand Body One (FSB-1)

The FSB-1 area is centrally located on the lower sand flat and is positioned approximately 180 m due west of the hardbottom reef and 153 m west of the moored instrumentation package. A very small area, compared to other sand bodies observed, this fine sand body demonstrated the greatest amount of net displacement, although it did not fall outside of the established 10 meter error tolerance buffer. From spring 2002 to fall 2002 the well-defined contact boundary swelled in nearly all compass directions expanding the areal extent of the sand body by more than 30% (Fig. 17B). Between fall 2002 and spring 2003 areal extent decreased slightly, but a high degree of displacement (146 m²) was observed in the northwest direction with little change in overall morphology of the sand body. The contact perimeter

Table 5. Displacement (m²) and net direction of movement of selected subareas located on lower sand flat adjacent to marine hardbottom reef. Percent change (grey shaded area) is the calculated displacement during the period divided by final area measured at the end of the period and normalizes the degree of change for comparative purposes. ND = no observed net directional component. Asterisk (*) denotes loss of NE corner of data due to nadir region during this period. # denotes sand body extends over nadir region for all surveys.

| | Spring '02 - Fall '02 3/14/02 - 11/21/02 | % Change | Fall '02 - Spring '03 11/21/02 - 5/30/03 | % Change | Spring '03 - Fall '03 5/30/03 - 10/14/03 | % Change |
|----------------------------|---|---------------------------|---|---------------------------|---|---------------------------|
| CSB-1 | 315 m ² ND | 7% | 438 m ² W-NW | 11% | 490 m ² E | 11% |
| CSB-2 | 233 m ² ND | 16% | 257 m ² ND | 15% | 152 m ² N/NE | 9% |
| FSB-1 | 62 m ² ALL ≠ E-NE | 15% | 146 m ² N-NW | 38% | 44 m ² SE | 13% |
| FSB-2 | 312 m ² ND* | 9% | 545 m ² N | 13% | 588 m ² ND | 15% |
| FSB-3 | 478 m ² S-SW | 7% | 384 m ² ND | 11% | 540 m ² ND | 22% |
| FSB-4[#] | 1378 m ² ND [#] | 9% | 750 m ² ND [#] | 5% | 832 m ² ND [#] | 7% |
| Average% Change | | 10.5 % | | 15.5% | | 12.8% |

between spring 2003 and fall 2003 demonstrated variable mobility along the eastern boundary with four small fingers emerging in the southeast, however, overall this same flank demonstrated no appreciable net movement (Fig. 17B). During this same period, the western and northern boundaries were shifted to the southeast approximately 1.5 to 2 m, but the remainder of the body remained stable. Overall, there was a clearly identifiable shift in the entire body to the northwest from the initial 2002 survey to the final fall 2003 survey. This migration, however, was deemed insignificant as it did not surpass the 10 meter buffer (Fig. 17B).

Coarse Sand Body Two (CSB-2)

The CSB-2 area is located approximately 75 m south-southwest of the low-relief hardbottom reef and approximately 100 m due south of the moored instrumentation. It is encompassed by a minimum of 30 m of surficial fine grain sand on all sides, which makes up the contact boundary. The extent of this body lies completely within line 6 of the sidescan surveys. Between the spring 2002 and fall 2002 surveys, this irregularly shaped body showed little organized displacement (Table 5, Fig. 18). However, the southeast contact shifted northwestward approximately 6-9 m while the remainder of the contact remained stable except for a small segment on the east flank, which also migrated west-southwest approximately 4 m. Further, the same southeast section as well as southwest contact flank expanded southward between the fall 2002 and spring 2002 surveys, while again the remainder of the coarse body experienced little change. The expansion ranged from approximately 3 m to more than 6 m. Overall, between the initial spring 2002 survey and final fall 2003 survey, there was minimal morphological change in both the shape and position of CSB-2 (Fig.18). Of significance, however, is the transient motion of the contact position itself, which seems to waver indiscriminately in conjunction with the sporadic mobilization of the fine-grained sediment

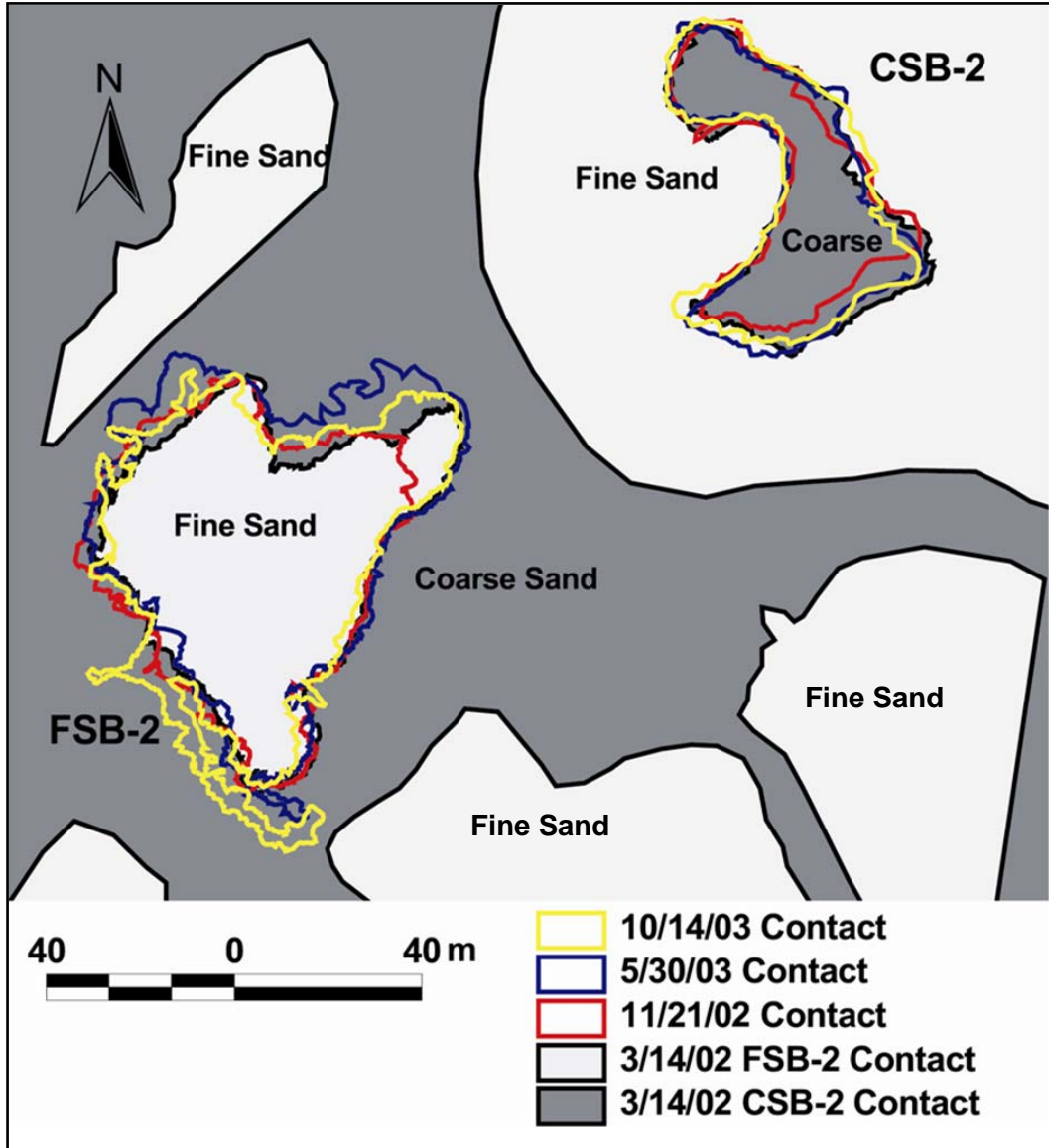


Fig. 18. CSB-2 and FSB-2 sand body contacts.

bordering the body. This is evidenced by the changes in areal extent from survey to survey, which ranged from a minimum of 1420 m² during the fall 2002 survey to a maximum of 1731 m² observed during the fall 2003 survey.

Fine Sand Body Two (FSB-2)

FSB-2 is located south of the FSB-1 and CSB-2 areas and approximately 176 m south of the nearest reef ledge. This area, contained completely on line 6 of the sidescan survey, showed no consistent change in net displacement over the course of the four surveys, however other notable morphologic changes were observed (Fig. 18). Initially, the contact observed in the spring 2002 survey between FSB-2 and the surrounding coarse-grained sediment was very well defined. From the initial survey to fall 2002, the contact remained stable along the eastern flank, yet an expansion of the contact perimeter between 0 to 5.5 m was observed across the remainder of the boundary. Total area increased slightly between these two periods, even though a small portion of the fall 2002 sand body was not digitized due to crossing of the nadir. In spring 2003, the areal extent of FSB-2 again swelled, increasing in coverage by over 17% from spring 2002 (Fig. 18). This expansion mainly occurred along the northern perimeter where this contact expanded northward from 0 to 15 m. The eastern flank remained stable, exhibiting almost no variability between surveys, while the southwestern flank also moved northward although in a rather inconsistent, highly variable pattern. Further, the spring 2003 survey exhibited the emergence of a narrow finger of fine sand protruding southeastward from the main southern contact boundary (Fig. 18). This same finger expanded southward in the fall 2003 survey and extended more than two thirds of the western contact perimeter. Additionally, the contact between spring 2003 and fall 2003 again was modified, but instead of expanding, this time the vast majority of the perimeter contracted, causing the areal extent of the body to diminish by

about 7%. Overall, there was no significant displacement during the nineteen-month period (Table 5)

Fine Sand Body Three (FSB-3)

The FSB-3 subarea positioned 540 m from the nearest reef edge is also the most southern sand body from the CORMP instrumentation, which is 741 m to the north-northwest. FSB-3 is 560 m southeast of CSB-2 and is contained entirely within line 8 of the sidescan surveys. Although no significant net displacement was observed between the spring 2002 and fall 2002 surveys (Table 5), FSB-3 expanded in area by more than 35% from its initial size of 2603 m² (Fig. 19A). This expansion, ranging from 0.5 to 7.75 m, occurred around the entire contact boundary except for a localized area in the northeast. Little morphological change occurred between the fall 2002 and spring 2003 surveys, and total area of the body remained constant. Similar to FSB-2, there was an emergence of a set of fingers in the southeast quadrant of the body, which were not apparent in the fall 2002 survey (Fig. 19A). Interestingly, these fingers grew in extent over the period leading up to the fall 2003 survey and evolved into a set of independent thinly veneered fine sand bodies covering the coarse-grained sediments contacting the boundary of FSB-3. The area of FSB-3 diminished 30% during the 5-month period between spring and fall 2003 surveys to 2490 m². From spring 2003 to fall 2003, there was a slight net displacement to the west of this body totaling 538 m², however, this shift did not exceed the error tolerance buffer (Table 5).

Fine Sand Body Four (FSB-4)

FSB-4 is the western most situated sand body in the study area, located 740 m west-southwest of FSB-2 and 930 m west-southwest of the moored instrument cage. This area is

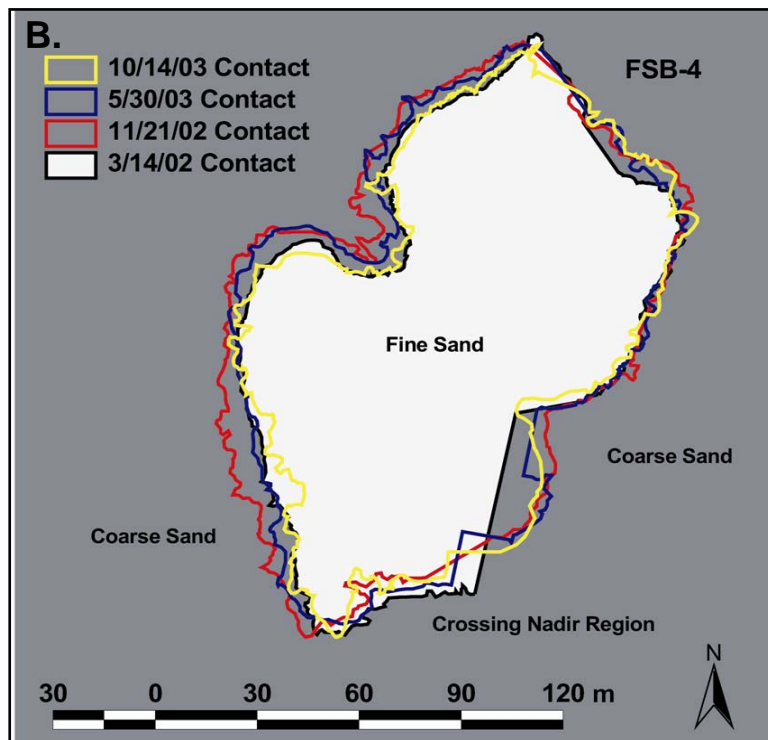
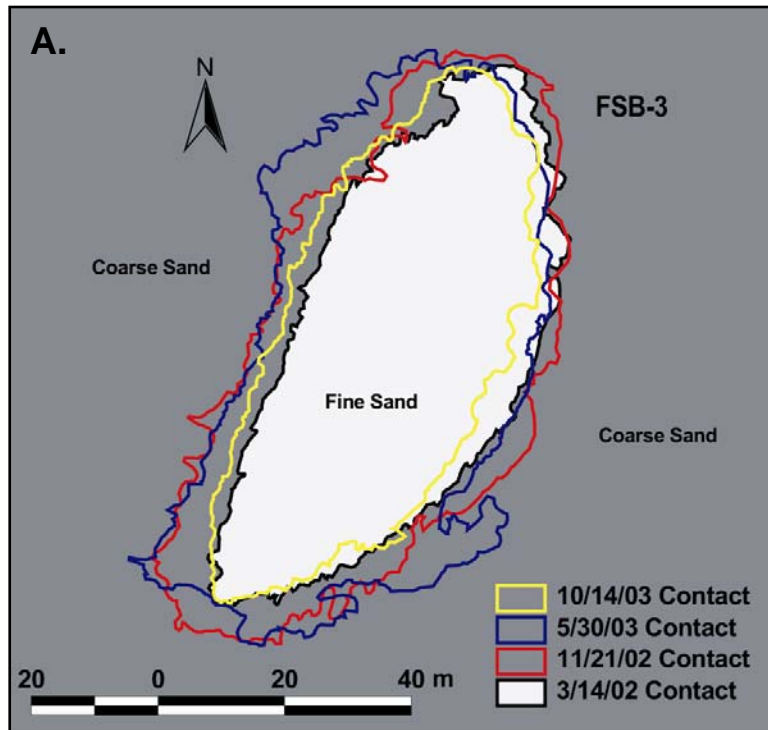


Fig. 19 FSB-3 and FSB-4 change detection analysis results.

located on line 8 of the sidescan survey and the eastern third of the FSB-4 crosses over the nadir region of the line swath, in effect limiting analysis results (Fig. 19B). The eastern contact displayed consistent expansion across its boundary ranging from 4 to 9.5 m between spring 2002 and fall 2002. From fall 2002 to spring, 2003 FSB2-3 exhibited little morphological change; however, the western boundary, which swelled between the previous two surveys, retreated to a similar position observed in spring 2002. Between spring 2003 and the final survey conducted in fall 2003, revealed further morphological change in the high and low backscatter contacts, specifically along the western boundary which continued to retreat eastward at variable rates ranging from about 1.0 to 7.5 m over the five-month time frame. The remainder of the contact showed little displacement and appeared rather stable. Overall, there were no significant changes that exceeded the established 10 m error tolerance buffers during the nineteen-month period between initial and final surveys. Further, due to the nadir region cutting directly across FSB-4, changes in area and net displacement reported in Table 5 are likely to be less reliable than previously discussed subareas.

DISCUSSION

Three physical processes active in the near-bed layer have been identified as the major forcing mechanisms responsible for mobilizing, suspending, and transporting sediment across the inner-shelf seabed in response to the broad spectrum of environmental surface conditions experienced in the Southern Atlantic Bight. Surface gravity waves and their associated near-bed orbital velocities, near-bottom mean currents dominated by low-frequency subtidal flows generated from surface winds, and slowly reversing tidal currents dominated by the M2 semidiurnal component all have measurable roles. These mechanisms are found to work synergistically with each other leading to the mobilization and minor transport of surficial fine

sand sized sediment in both the along- and across-shelf directions. It is clear that sediment transport occurring at this inner-shelf location is primarily driven by a complex combination of wave-current interactions of the aforementioned variables similar to those first noted by Grant and Madsen (1979).

Four classes of meteorological events were identified as initiating significant periods of sediment mobility throughout the nineteen-month duration of study. Tropical storms, extratropical low pressure areas including nor'easters, air mass boundaries and associated fronts, as well as fair-weather southerly wind events all played contributing roles in elevating local sea state and local winds for several hours to days, ultimately resulting in high-energy sea bottom conditions required for moving unconsolidated seabed material. Four tropical events occurred during the nineteen-month period of study and were found to be the most influential class of events on record. Back to back occurrence of two moderate to strong tropical systems over a sixteen-day period in September 2003 is believed to be responsible for effectively shifting large quantities of sediment and drastically changing the sedimentation pattern between two similar seasonal periods within the study.

Data presented in this paper illustrate that near-bottom conditions at this discrete inner-shelf site are frequently energetic enough to agitate sediment as bedload and very often incipiently suspend fine-grained sand in response to a wide range of surface weather events. Model output from the Styles and Glenn (2002) boundary layer model indicate that conditions fall below critical values for no movement approximately 33.9% of the time. The remaining periods were dominated by bedload movement approximately 16.6% of the time and upon higher energy conditions as incipiently suspended load more than 48.9% of the time. Conditions required for full suspension of the fine sand material were very rare and found to occur during

less than 1% of the study period. Of this 1%, 72% occurred during the passage of Hurricane Isabel. Coarse grain sediments are believed to be only weakly mobile under even the most extreme conditions and were not found to be moved significantly during the course of study.

Interestingly, however, upon first visual inspection, high-resolution sidescan sonar imagery of the seafloor reveal that over the study period conditions did not favor mass exchanges of sediment in the along-shelf and across-shelf directions such that the gross morphology of the seabed is markedly modified. These findings are similar to Thielert et al. (2001) who saw no significant changes in the distribution of fine and coarse sands in repeat high-resolution sidescan sonar surveys (Klein 100 kHz) of the lower shoreface offshore of Wrightsville Beach over a three-year period consisting of normal climatological conditions. Thielert et al. (2001) suggested that “typical” storms and other high-energy events do not result in large-scale changes to the limited veneer of fine sediments available for transport. Rather, the unconsolidated fraction of the seabed appears to be relatively stable even under the stress of physical forcing mechanisms produced in response to several high-energy events over the course of a nineteen-month period with little change in shape and location. Findings here, as defined by the established error tolerances, also shows there was only a limited degree of significant net directional transport observed amongst the six sites examined. However, in the five to seven month periods between repeat surveys, it was common to see the areal extent of the sand bodies substantially expand and contract, or to have fingers of fine sand material simultaneously emerge, migrate short distances, only later to be winnowed away elsewhere on the inner-shelf.

A conceptual model composed of a two-tiered data matrix was developed to better constrain the long-term effects physical processes acting in the near-bottom have on the distribution of surficial sediments. In this model, the twenty-three sediment mobility events

identified and their defining characteristics were clustered according to occurrence with respect to the biannual acquisition dates of sidescan sonar (Table 6). Further examination of the six sand body subareas focused on collective changes in sedimentation patterns for the periods between sidescan cruises rather than individual changes in displacement and net direction of movement. Several interesting results were produced by this analysis comparison.

During the period between March 14 to November 21, 2002 (hereafter 2002 spring-fall), which are the respective dates high-resolution sonar imagery were acquired, a 7 to 18% decrease in the areas of the two coarse sand bodies was observed, while each of the four fine sand bodies probed exhibited a substantial increase in area. Conversely, the reverse was true for a similar period of time just one year later between May 30 and October 14, 2003 (2003 spring-fall). During the 2003 spring-fall period, the coarse sand bodies gained area, while each of the fine sand sheets examined were significantly reduced in size. The intermediate period between November 21 to May 30 showed little consistent pattern in areal change and will not be discussed further in great detail (Table 6A).

Focusing first on the spring-fall 2002 period, eight sediment mobility events were recorded, including two events associated with weak to moderate tropical events. Maximum wave-current shear velocities exceeded full suspension limits for a maximum of one eight hour period during Tropical Storm Gustav, otherwise the primary mode of sediment transport during the high-energy events of this period was incipient suspended load and bedload. These modes of transport are believed to be driven principally by waves and their associated near-bed wave orbital velocities. Although several strong wind events did occur, subtidal currents in the near-bed layer remained weak and played a minor part in redistributing sediment. Maximum subtidal

Table 6. Conceptual model comparing area analysis of six subareas examined during biannual sidescan sonar results to frequency, distribution, and intensity of high-energy sediment mobility events. High-energy events are clustered according to the corresponding time between repeat surveys. Cells highlighted in blue in Table 6A represent a positive increase in sand body area while orange reflects a net decrease in sand body area. In Table 6B, u_{*cw} values highlighted in bold indicate the critical threshold for full suspension of fine-grained material was exceeded. Duration = time (hr) ABS signal is above criteria level and. Subtidal magnitude, u_b , and u_{*cw} are each given in cm sec^{-1} .

Table 6A. % Change in Sand Body Area between Repeat Sidescan Surveys

| | Spring 2002 - Fall 2002 3/14/02 - 11/21/02 | Fall 2002 - Spring 2003 11/21/02 - 5/30/03 | Spring - Fall 2003 5/30/03 - 10/14/03 |
|--------------|---|---|--|
| CSB-1 | -7% | -14% | +15% |
| CSB-2 | -18% | +17% | +5% |
| FSB-1 | +31% | -9% | -14% |
| FSB-2 | +3%* | +18% | -7% |
| FSB-3 | +36% | +1% | -30% |
| FSB-4 | +14.8% | -6% | -8% |
| Avg. | 18.3 % | 10.8% | 13.2% |

Table 6B. Sediment Mobility Event Characteristics

| | #1 | #2 | Gu | #4 | Ky | #6 | #7 | #8 | #1 | #2 | #3 | #4 | #5 | #6 | #7 | #8 | #9 | #1 | #2 | He | Is | #5 | #6 |
|-------------------------------|------|------|------------|------|-------|-------|-------|-------|------|-------|------|------------|------|------|--------|------|------|------|------|------------|------------|------|------|
| Type | ETlo | ETlo | T | ETf | T | ETlo | ETf | ETlo | ETf | ETlo | ETf | ETlo | ETlo | ETf | ETf | ETf | ETlo | ETsw | ETsw | T | T | ETf | ETf |
| Duration | 29 | 42 | 24 | 6 | 19 | 22 | 12 | 13 | 10 | 11 | 11 | 53 | 16 | 8 | 22 | 7 | 11 | 18 | 12 | 23 | 79 | 23 | 14 |
| Subtidal Along | SW | SW | SW | SW | SW-NE | SW | SW | NE | SW | SW-NE | NE | NE | SW | NE | SW-NE | SW | SW | NE | NE | SW | SW-NE | NE | SW |
| Subtidal Across | off | off | off | off | off | off | off | on | on | on | on | on | off | on | off-on | on | off | on | on | on | off-on | on | off |
| Subtidal Max. | 15.1 | 12.0 | 9.8 | 7.4 | 6.0 | 8.3 | 13.3 | 7.2 | 7.0 | 14.8 | 8.9 | 12.2 | 5.2 | 7.9 | 9.0 | 7.1 | 7.7 | 10.9 | 9.2 | 11.0 | 19.7 | 9.9 | 11.6 |
| H_s Approach | E-SE | E-SE | E-SE | E-SE | E-SE | NE-SE | NE-SE | SE-NE | S | SE-S | SE-S | S-E | E-SE | SE | S-SE-S | E-SE | SE | SE-S | S | SE-E | SE-E-N | SE-E | S |
| u_b Max. | 24.7 | 31.6 | 37.5 | 30.8 | 18.9 | 23.7 | 22.5 | 14.3 | 32.9 | 24.2 | 15.0 | 42.9 | 20.5 | 26.3 | 21.7 | 18.1 | 27.5 | 23.4 | 11.0 | 43.2 | 63.9 | 23.1 | 26.1 |
| u*_{cw} Max. | 5.1 | 6.0 | 6.4 | 5.8 | 4.5 | 5.0 | 4.9 | 4.1 | 6.0 | 5.0 | 4.1 | 7.0 | 4.6 | 5.3 | 4.8 | 4.4 | 5.5 | 5.1 | 3.9 | 7.1 | 8.6 | 5.0 | 5.3 |

current velocities ranged from 6 to 15 cm sec⁻¹ for the eight recorded events and were generally directed to the southwest in the along-shelf direction.

The observed sedimentation pattern reflects both the near-bottom hydrodynamic conditions during high-energy periods and the surficial geology of a sediment starved seabed. The “patchy” cover of fine sand present on the lower shoreface and inner-shelf of Onslow Bay is limited and composed of a finite volume of material of thicknesses on the order of 50 cm or less (Thieler, et al. 1995). The fine sand sheets are typically linear to slightly irregular with little relief, however, it is expected that the maximum thicknesses are central to the body and thin to a fine veneer at their edges as they transition into the less mobile gravelly coarse sand bodies present as a lag pavement. During extensive periods of mobilization, fine sands central to the bodies are effectively spread outward by the oscillatory motions produced via near-bottom wave orbitals. In the process of being mobilized as bedload and incipient suspended load, the fine sands spill overtop adjacent immobile coarse-based pavement areas and are deposited as normal bottom conditions ensue. Diver collected boxcores obtained throughout this research exhibit instances of fine sands (<10 cm typically) overlying coarse-grained materials (Fig. 20). Thieler et al. (2001) also inferred a similar process around the edges of ripple scour depressions inshore of this location. The authors also noted that the large megaripple crests associated with coarse material were able to be identified below the overlying fine sand laterally for several meters. Overall, the net effect of the hydrodynamic regime associated with high-energy sediment mobility events during the 2002 spring-fall period was to substantially increase the area of the fine sand bodies and simultaneously diminish the total area of adjacent surfaces consisting of poorly sorted coarse-grained material.

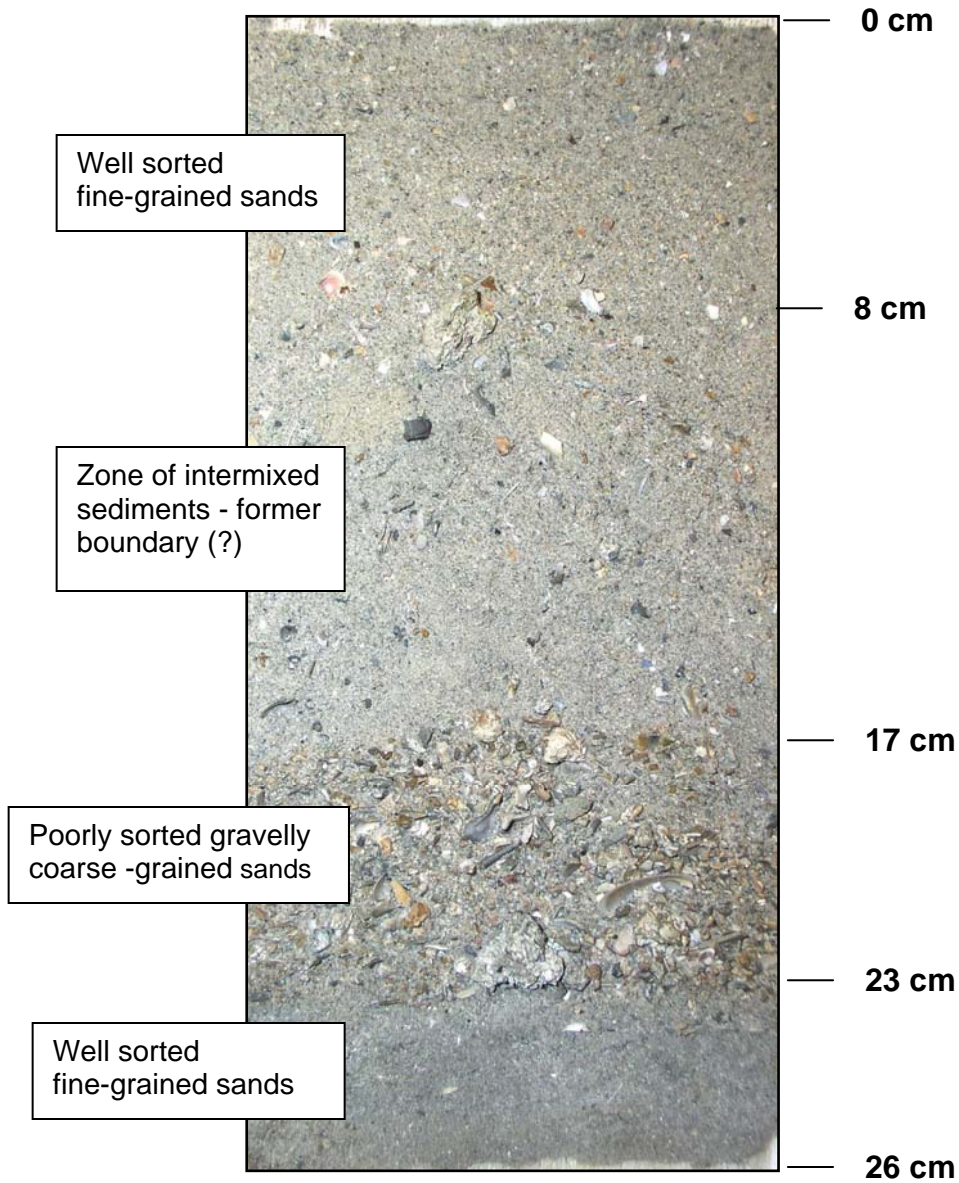


Fig. 20. Sediment relief peel produced from diver collected boxcore obtained approximately 30 m south of OB3M instrumentation cage. This peel demonstrates the mobility of fine sands overtopping and infilling less mobile adjacent coarse sand body areas. Core length is approximately 26 cm.

During the 2003 spring-fall period, the sedimentation pattern is much different than that observed during the 2002 spring-fall period. The two coarse-grained sand bodies increased in area by an average of 10% whereas the four fine-grained sand bodies exhibited a 15% average decrease in area. During this period, a total of six events were identified, including the two strongest events recorded, Tropical Storm Henri and Hurricane Isabel, which impacted the region over the sixteen day period beginning September 3 and ending on September 19. As Table 6B shows the majority of storm parameters between the two periods are comparable in magnitude and direction.

The only significant difference between the two periods is the mode of sediment transport achieved in response to the available energy in the near-bottom. The 2003 period experienced an extended episode of sediment mobility yielding full suspension conditions during the height of Hurricane Isabel. For forty-eight consecutive hours beginning at 0000 UTC on September 16, combined wave and current shear velocities exceeded critical thresholds required for full suspension of fine sands (Fig. 13F). Additionally, during the preceding 20 hours prior to this period, u_{*cw} values averaged 5.9 cm sec^{-1} , which is just below full suspension criteria and well above six of the eight maximum values observed for all sediment mobility events occurring during the 2002 spring-fall period (Table 6B).

A sediment tube attached 23 cm above the seabed to the instrumentation cage at the OB3M site during the research provides further evidence of the tremendous impact Isabel had on the seabed and suspension of bottom sediments. In the six-month period from March 2002 to June 2003, 205.4 g of sediment were collected for a sedimentation rate of approximately 58 g-mos^{-1} . During the three-month period from July to late September 2003, 512.4 g of sediment

were obtained for a sedimentation rate of over 204 g-mos^{-1} (Fig. 21). Mean grain size calculated for this material was 0.2370 mm for the pre-Isabel period and 0.2085 mm for the time bracketing Hurricane Isabel. In both cases, the material is classified texturally as moderately sorted fine sand. Given this information, this is an extreme event unlike that recorded elsewhere throughout the duration of this research.

Widespread suspension of the fine-grained fraction during this solitary extreme event had a substantial effect on the unconsolidated surface cover. Although the resulting suspension did not support net transport of entire fine sand bodies in a given compass direction as was expected, the processes at work did act to modify the contact boundaries where fine and coarse-grained sand bodies meet. This is evident in the sedimentation pattern that completely reversed itself from the 2002 spring-fall season (Table 6A). As stated earlier, fine sands form only a thin cover overtop the coarse grain pavement lag. This is especially true around the perimeters of these bodies where the fines intermix and transition into areas composed primarily of coarse-grained material. Under full-suspension conditions, fine sands were effectively winnowed away from these areas where they were only sparse in cover at the onset. At the conclusion of the event, the result was that much of the material that had composed the thin veneers near the contact edges was swept away later to be redeposited elsewhere on the shelf. As Table 6B illustrates, the two coarse-grained subareas examined here gained area due to this sweeping action of the fines, while fine sand bodies lost area as their edges were winnowed away during the period of full-suspension. These findings concur with the qualitative study of Backstrom (2002), which examined the storm-driven sedimentary changes in the lower shoreface and inner-shelf region offshore of Kure Beach, North Carolina (approximately 14 km southwest of this study area). Visual examination of two sidescan sonar mosaics did not reveal significant sedimentary changes

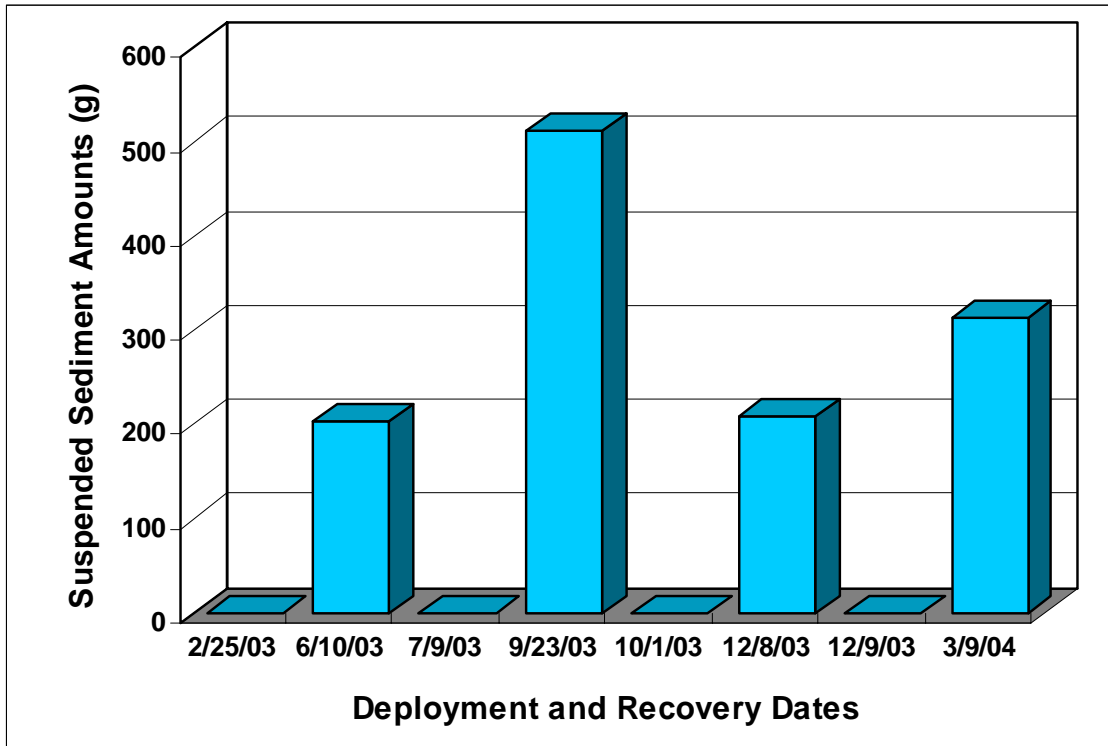


Fig. 21. Bar graph showing distribution of suspended sediment amounts obtained in a sediment cup positioned 23 cm above the seabed and mounted vertically to the OB3M instrumentation cage. Note the peak during the period including the passage of two strong tropical events (Tropical Storm Henri and Hurricane Isabel) during September 2003. March 2003 was the initial deployment date of the sediment cup.

before and after the passage of hurricanes Dennis and Floyd (1999). However, on a smaller scale there were regions of noticeable differences in acoustic backscatter suggesting minor changes in grain size texture and spatial distribution. Over the region of study, a reduction of fine-grained unconsolidated sediments was compensated for by new exposures of low-relief marine hardbottom reefs that were not visible prior to storm activity (Backstrom, 2002). It is conceivable that without an extreme high energy similar to Isabel, the distribution of sediment cover across the study region would have likely resembled that of the preceding 2002 spring-fall period.

One potential caveat to this scenario is the discrepancy between the duration of the two repeat sonar surveys being compared. The 2002 spring-fall period encompasses a larger portion of time than the 2003 spring-fall period and accounts for a period of time that would be climatologically more active (early spring and later fall). Further, wave and current data, and thus our sediment mobility event identifying criteria extend back to only April 25, 2002, while the first sidescan sonar period begins on March 14, 2002. Review of wind, wave and atmospheric pressure data from the FPT C-Man station between March 14 and April 25 suggested the occurrence of two more weak events during this period that had the potential to mobilize sediment. It was concluded, however, that these events were likely to be of little consequence based on the specific meteorological data.

CONCLUSIONS

High-energy events play a major role in the mobilization of sediment on the inner-continental shelf of Onslow Bay and are produced in response to a variety of meteorological and oceanographic processes. These processes are manifested within the near-bottom layer as a combination of three dominant physical forcing mechanisms, all with a contributing role in

initiating and sustaining sediment transport within the inner-shelf region. Semidiurnal tidal currents, waves and corresponding near-bottom wave orbitals, as well as mean currents dominated by wind-generated subtidal flows work in conjunction with one another to induce stress on the surficial seabed and exceed critical thresholds for mobilizing sediment. The fine-grained sediment fraction of the seabed is frequently agitated even under average fair-weather conditions.

For all events, the dominant mechanism for mobilizing and vertically mixing sediments into suspension is increased bed shear stress due to wave orbital action. Subtidal currents, although elevated well above ambient levels during intense wind events to velocities exceeding 15 cm sec^{-1} remained weak in comparison to wave inputs and play only secondary roles. According to critical shear velocity values calculated for the fine sand portion of the seabed, material with a mean grain size of less than 0.2041 mm was mobilized more than 66% of the time over the nineteen month period in response to the combined effects of near-bottom wave and current interactions. During higher-energy events, fine sand is often mobilized through a combination of bedload and incipiently suspended load, and less frequently via fully suspended load, which accounted for less than one percent of the total time sediment was in motion.

Twenty three sediment mobility events were identified consisting of a broad range of intensities and durations. A generalized classification system based on common meteorological events observed across the region demonstrates that over the nineteen-month period of study extratropical low pressure areas most frequently initiated a seabed response. In a normal climatological year, these would include several nor'easter type storms, which in the past have been observed to be quite influential in transporting large quantities of sediment across inner-shelf regions. However, during the time frame of this research, there were no major nor'easters

recorded off the southeast North Carolina coast. In general, there were eight occurrences of events where closed isobar areas of low pressure and associated frontal boundaries directly influenced the region, seven involving the passage of frontal boundaries, two fair-weather southerly winds events and four tropical systems.

Repeat high-resolution sidescan sonar surveys obtained over the same time, however; provide evidence that interannual changes to the sedimentation pattern of this sediment starved inner-shelf region were only significantly influenced by the occurrence of a singular tropical born storm system that impacted the shelf waters of Onslow Bay in September 2003. Hurricane Isabel elevated near-bottom wave orbital velocities to more than six times their fair-weather average and caused full-suspension of sediment for more than forty eight consecutive hours. This accounted for more than 72% of the full suspension conditions observed during the entire March 2002 to October 2003 period and was observed nowhere else in the record of study. Thus, the occurrence of several lesser storms of moderate energy, that are climatologically higher in frequency, but less intense are less likely to change the distribution and gross morphology of limited amount of surficial sediment cover that exists at this inner-shelf location. This is in relation to the occurrence of a sole extreme event, such as Hurricane Isabel, that is several times more intense and impacts the region for only a fraction of the time as all other events combined. Although the overall gross morphology and sediment distribution remained relatively unchanged even after the passage of Isabel, changes in shape, size, and orientation of six observed sand bodies did occur and were most changed after the passage of this one extreme event.

REFERENCES

- Backstrom, J.T., 2002. Storm-driven sedimentary changes on the shoreface of a replenished beach: Kure Beach, North Carolina. M.S Thesis, University of North Carolina at Wilmington, Wilmington, NC, 50 pp., unpublished.
- Blackwelder, B.W., Macintyre, I.G. and Pilkey, O.H., 1982. Geology of the continental shelf, Onslow Bay, North Carolina, as revealed by submarine outcrops. AAPG Bull., 66: 44-56.
- Beavers, R.L., 1999. Storm Sedimentation on the surf zone and inner continental shelf, Duck, NC. Doctoral dissertation, Duke University, Durham, North Carolina, 117 pp., unpublished.
- Deines, K.L., 1999. Backscatter estimation using broadband acoustic doppler current profilers. Oceans '99 MTS/IEEE Conference Proceedings, 13-16.
- Grant, W.D. and Madsen O.S., 1979. Combined wave and current interaction with a rough bottom. Journal of Geophysical Research, 84 (C4), 1797 – 1808.
- Hayes, M.O., 1979. Barrier island morphology as a function of tidal and wave regime, in Leatherman, S.P., ed., Barrier Islands: From the Gulf of St. Lawrence to the Gulf of Mexico: New York, Academic Press, p. 1-27.
- Jarrett, J.T., 1977. Sediment budget analysis, Wrightsville Beach to Kure Beach, North Carolina. Proc. Coastal Sediments '77. ASCE, New York, pp. 986-1005.
- Middleton, G.V., 1984. Mechanics of Sediment Movement: Lecture Notes for Short Course No. 3. Chapter 6 pp.216-230 Society of Economic Paleontologists and Mineralogist Publication, 1984. 401 pp.
- Milliman, J.D., Pilkey, O.H., and Ross, D.A., 1972. Sediments of the continental margin off the eastern United States. Geol. Soc. Am. Bull., 83, 1315-1334.
- Niedoroda A.W., Swift D.J., and Hopkins T.S., 1985. The shoreface. Coastal Sedimentary Environments. Ed. Richard A. Davis Jr., New York: Springer-Verlag, 533-623.
- Pietrafesa, L.J., Janowitz, G.S., Wttman, P.A., 1985. Physical oceanographic processes in the Carolina Capes, In: Oceanography of the Southeastern U.S. Continental Shelf, 23-32.
- Pearson D.K., Riggs, S.R., 1981. Relationship of surface sediments on the lower forebeach and nearshore shelf to beach nourishment at Wrightsville Beach, North Carolina. Shore and Beach, 49, 26-31.
- Renaud, P.E., Ambrose, Jr., W.G., Riggs, S.R., Syster, D.A., 1996. Multi-level effects of severe storms on an offshore temperate reef system: Benthic sediments, macroalgae, and implications for fisheries. Marine Ecology 17, 383-401.

- Renaud, P.E., Riggs, S.R., Ambrose Jr., W.G., Schmid, K., Snyder, S.W., 1997. Biological-geological interactions: storm effects on macroalgal communities mediated by sediment characteristics and distribution. *Continental Shelf Research* 17(1), 37-56.
- Riggs S.R., Snyder S.W., Hine A.C., Mearns D.L., 1996. Hardbottom morphology and relationship to the geologic framework: Mid-Atlantic Continental Shelf. *J. Sedimentary Research*, 66(4), 830-846.
- Schmid, K.A., 1996. Patterns of sedimentation associated with hardbottom habitats on the North Carolina margin. M.Sc. Thesis, East Carolina University, Greenville, NC, 161 pp., unpublished.
- Styles, R. and Glenn, S.M., 2000. Modeling stratified wave and current bottom boundary layers on the continental shelf. *Journal of Geophysical Research*, 105 (C10), 24119-24139.
- Thieler, R.E., Brill, A.L., Cleary, W.J., Hobbs C.H., Gammisch, R.A., 1995. Geology of the Wrightsville Beach, North Carolina shoreface: implications for the concept of shoreface profile equilibrium. *Marine Geology*, 126, 271-287.
- Thieler, E.R., 1996. Shoreface processes in Onslow Bay. In W.J. Cleary (editor), *Environmental Coastal Geology: Cape Lookout to Cape Fear, NC*. Carolina Geological Society, 23-32.
- Thieler, E. R., Gayes, P.T., Schwab, W.C., and Harris M.S., 1999. Tracing sediment dispersal on nourished beaches; two case studies. In: N.C. Kraus, W.G. McDougal (editors), *Coastal sediments '99: Proceedings of the International Symposium on Coastal Engineering and Science of Coastal Sediment Processes*, ASCE, Reston, 3, 2118-2136.
- Thieler, E.R., Schwab, W.C., Pilkey, O.H., and Cleary, W.J., 2001. Modern sedimentation on the shoreface and inner-shelf at Wrightsville Beach, North Carolina. *Journal of Sedimentary Research* 71(6), 958-970.
- Wave Information Studies (WIS) Research. Website: <http://frf.usace.army.mil/wis/> Maintained by the Coastal and Hydraulics Lab, U.S Army Corps of Engineers. Accessed 6/24/2004.
- Williams, J.J. and Rose, C.P., 2001. Measured and predicted rates of sediment transport in storm conditions. *Marine Geology* 179, 121-133.
- Wren, P. A. and Leonard L. 2004. Sediment transport during Hurricane Isabel on the mid-continental shelf in Onslow Bay, North Carolina. *Estuarine, Coastal, and Shelf Science* (in press).
- Wright, L.D., Boon, J.D., Green, M.O., List, J.H., 1986. Response of the mid-shoreface of the southern Mid-Atlantic Bight to a "northeaster." *Geo-Marine Letters*, 6, 153-160.
- Wright, L.D., 1987. Shelf-surfzone coupling: diabathic shoreface transport. *Proceedings from Coastal Sediments '87*. ASCE, New York, pp. 25-40.

Wright, L.D., Boon, J.D., Kim, S.C., List J.H., 1991. Modes of cross-shore sediment transport on the shoreface of the Middle Atlantic Bight. *Marine Geology*, 96, 19-51.

Wright, L.D., 1993. Micromorphodynamics of the inner continental shelf: a Middle Atlantic Bight case study. *Journal of Coastal Research* (special issue), 15, 93-120.

Wright, L.D., Xu, J.P., Madsen, O.S., 1994. Across-shelf benthic transports on the inner-shelf of the Middle Atlantic Bight during the "Halloween storm" of 1991. *Marine Geology*, 118, 61-77.

Wright, L.D., Kim, S.C., Friedrichs, C.T., 1999. Across-shelf variations in bed roughness, bed stress, and sediment suspension on the northern California shelf. *Marine Geology*, 154, 99-115.

Wright, L.D., 1995. *Micromorphodynamics of inner continental shelves*. CRC Press, Boca Raton, 241 pp.

Xu, J.P., Wright, L.D., 1998. Observations of wind generated currents of Duck, North Carolina. *Journal of Coastal Research* 14, 610-619.

APPENDICES

Appendix A: 2002 sediment mobility events recorded from June through December 2002. # - limited data due to equipment failure. Etlo = extratropical low pressure area; T = tropical born system; ETf = extratropical frontal boundary; BH = southerly wind event. Events denoted by an asterisk are highlighted in the Results section

| 2002 Events | Type | Winds (knots) | H _s (m) | T _p (sec) | u _b (cm s ⁻¹) | ABS (dB) | Mean current (cm s ⁻¹) | Subtidal current (cm s ⁻¹) | u* _c (cm s ⁻¹) | u* _{cw} (cm s ⁻¹) |
|--------------------|------|-------------------|--------------------|----------------------|--------------------------------------|----------|------------------------------------|--|---------------------------------------|--|
| 1. 5/4 -5/6 | ETlo | 5-33 All | 0.7 - 2.4 | 5 - 9 | 0.1 - 24.7 | 56 - 69 | 0.2 -18.0 | 2.5 - 15.1 | 0.1 - 1.5 | 0.3 - 5.1 |
| 2. 5/22 - 5/25 | ETlo | 5-35 NE-W-SW | 0.6 - 2.3 | 5 - 12 | 2.1 - 31.6 | 59 - 69 | 0.3 - 16.8 | 1.6 - 12.0 | 0.2 - 1.5 | 1.4 - 6.0 |
| 3. 9/8 - 9/13* | T | 10-40 NE-NW-NE | 0.5 - 2.0 | 5 - 10 | 1.7 - 37.5 | 55 - 69 | 1.8 - 13.8 | 2.8 - 9.8 | 0.2 - 1.3 | 1.3 - 6.4 |
| 4. 9/30 - 10/2 | ETf | 10-25 N-E | 0.8 - 1.6 | 5 - 11 | 2.9 - 30.8 | 59 - 67 | 0.4 - 10.0 | 1.9 - 7.4 | 0.2 - 1.0 | 1.6 - 5.8 |
| 5. 10/10 -10/14 | T | 10-35 NE-S-N | 0.6 - 2.2 | 5 - 10 | 1.6 - 18.9 | 60 - 68 | 0.3 - 11.0 | 3.3 - 6.0 | 0.1 - 0.8 | 1.1 - 4.5 |
| 6. 10/22 - 10/24 | ETlo | 5-20 N-NE | 0.7 - 1.1 | 5 - 11 | 0.2 - 23.7 | 59 - 79 | 1.1 - 11.4 | 3.1 - 8.3 | 0.2 - 0.9 | 0.4 - 5.0 |
| 7. 11/6 - 11/8 | ETf | 10-40 S-W-N | 0.7 - 1.7 | 4 - 11 | #2.5 - 22.5 | 59 - 68 | 0.5 - 16.7 | 3.8 - 13.3 | #0.5 - 1.2 | #1.9 - 5.9 |
| 8. 11/12 - 11/14 | Etlo | 5-40 SE-SW-N | 0.9 - 1.5 | 4 - 18 | 0.2 - 14.3 | 59 - 68 | 0.9 - 11.6 | 3.2 - 7.2 | 0.2 - 0.9 | 0.4 - 4.1 |
| 9. 12/20 - 12/22 | ETf | 19-41 SE-W | 0.7 - 1.9 | 5 - 10 | 8.2 - 32.9 | 59 - 68 | 0.9 - 15.4 | 2.7 - 7.0 | 0.3 - 0.9 | 3.0 - 6.0 |
| 10. 12/25 - 12/27* | ETlo | 15-35 SE-NW | 0.6 - 1.8 | 6 - 9 | 6.0 - 24.2 | 59 - 68 | 0.7 - 17.1 | 4.1 - 14.8 | 0.2 - 1.5 | 2.6 - 5.0 |

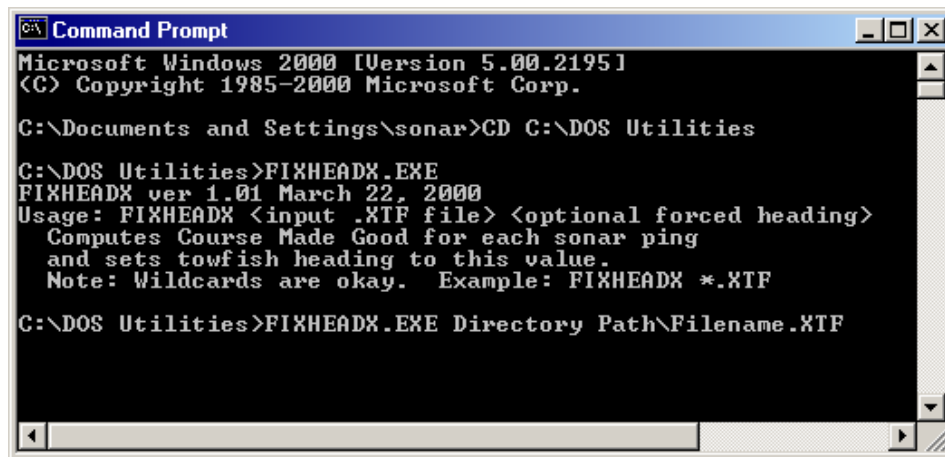
2003 sediment mobility events. Data below are recorded from January through October 2003. # - limited data due to equipment failure. Etlo = extratropical low pressure area; T = tropical born system; ETf = extratropical frontal boundary; BH = southerly wind event. Events denoted by an asterisk are highlighted in the Results section.

| 2003 Events | Type | Winds (knots) | Hs (m) | T _p (sec) | u _b (cm s ⁻¹) | ABS (dB) | Mean current (cm s ⁻¹) | Subtidal current (cm s ⁻¹) | u* _c (cm s ⁻¹) | u* _{cw} (cm s ⁻¹) |
|------------------|------|------------------|------------|----------------------|--------------------------------------|----------|------------------------------------|--|---------------------------------------|--|
| 1. 2/4 - 2/6 | Etf | 10-40 S-N | #1.0 - 1.5 | 3 - 11 | #15.0 | 57 - 69 | 1.1 - 12.1 | 3.7 - 8.9 | #1.0 | #4.1 |
| 2. 2/23 - 2/27 | Etlo | 15-50 S-N-SE | 0.7 - 2.1 | 4 - 11 | 1.9 - 42.9 | 61 - 72 | 1.3 - 17.8 | 4.0 - 12.2 | 0.2 - 1.4 | 1.5 - 7.0 |
| 3. 3/16 3/18 | Etlo | 5-30 ALL | #0.8 - 2.0 | 3 - 10 | #6.0 - 20.5 | 58 - 68 | 0.2 - 8.9 | 3.1 - 5.2 | #0.3 - 0.8 | #2.8 - 4.6 |
| 4. 3/21 - 3/23 | Etf | 8-33 SE-W | #0.6 - 1.6 | 3 - 9 | #6.5 - 26.3 | 56 - 68 | 0.6 - 13.6 | 3.1 - 7.9 | #0.1 - 1.3 | #2.5 - 5.3 |
| 5. 4/6 - 4/9 | Etf | 10-35 ALL | 0.6 - 2.1 | 3 - 11 | 0.2 - 21.7 | 56 - 70 | 1.3 - 14.7 | 4.1 - 9.0 | 0.2 - 1.1 | 0.9 - 4.8 |
| 6. 4/25 - 4/27 | Etf | 10 -38 SE-W | 0.6 - 1.9 | 4 -10 | 2.4 -18.1 | 50 - 68 | 0.4 - 10.4 | 2.4 - 7.1 | 0.2 - 1.0 | 1.4 - 4.4 |
| 7. 5/23 - 5/25 | ETlo | 5-30 SE-NW | 0.8 - 1.9 | 5 - 13 | 2.4 - 27.5 | 55 - 68 | 0.7 - 11.4 | 2.3 - 7.7 | 0.1 - 1.1 | 1.4 - 5.5 |
| 8. 6/7 - 6/10* | BH | 10-30 SE-SW | 0.7 - 1.6 | 6 - 9 | 4.0 - 23.4 | 54 - 67 | 0.7 - 14.1 | 1.4 - 10.9 | 0.3 - 1.2 | 1.9 - 5.1 |
| 9. 7/23 - 7/25 | BH | 18-28 S-SW | 1.0 - 1.5 | 4 - 10 | 0.2 - 11.0 | 63 - 68 | 1.8 - 11.8 | 6.2 - 9.2 | 0.7 - 1.2 | 0.8 - 3.9 |
| 10. 9/5 - 9/12 | T | 10-38 SE-N-NW | 0.7 - 2.2 | 5 - 16 | 2.1 - 43.2 | 59 - 70 | 0.1 - 18.0 | 1.8 - 11.0 | 0.1 - 1.5 | 1.3 - 7.1 |
| 11. 9/15 - 9/20* | T | 10-60 SE-N-SW | 1.0 - 2.5 | 5 - 18 | 1.2 - 63.9 | 58 - 73 | 0.2 - 26.1 | 1.9 - 19.7 | 0.2 - 2.1 | 1.1 - 8.6 |
| 12. 9/28 - 9/30 | Etf | 10-25 SW-N | 0.5 - 1.5 | 5 - 14 | 4.5 - 23.1 | 57 - 70 | 0.7 - 13.3 | 2.9 - 9.9 | 0.2 - 1.0 | 2.2 - 5.0 |
| 13. 10/7 - 10/11 | Etf | 10-28 E-N | 0.7 - 1.7 | 4 - 12 | 2.7 - 26.1 | 57 - 68 | 0.5 - 15.9 | 2.5 - 11.6 | 0.3 - 1.3 | 1.7 - 5.3 |

Appendix B: Instructions for Using ISIS and DelphMap Side-scan processing software

Navigation Correction

1. Raw .XTF files are first modified using FIXHEADX.exe DOS utility. This utility computes course made good for each sonar ping and sets the towfish heading to this new value. See Chapter 4: *DOS Utilities for Isis Data* of DELPHS Utilities Manual for more information regarding this script. Note: Once the script is run, original data heading data is overwritten with new towfish heading values.



```
Microsoft Windows 2000 [Version 5.00.2195]
(C) Copyright 1985-2000 Microsoft Corp.

C:\Documents and Settings\sonar>CD C:\DOS Utilities

C:\DOS Utilities>FIXHEADX.EXE
FIXHEADX ver 1.01 March 22, 2000
Usage: FIXHEADX <input .XTF file> <optional forced heading>
Computes Course Made Good for each sonar ping
and sets towfish heading to this value.
Note: Wildcards are okay. Example: FIXHEADX *.XTF

C:\DOS Utilities>FIXHEADX.EXE Directory Path\Filename.XTF
```

Replaying of Data File

1. Open *Isis Sonar v.6*. In the main window, choose FILE > PLAYBACK. In the Disk or Playback box choose “Disk Playback.”
 - a. All side-scan data for inner-shelf study site resides on F- disk > 5 Mile > cruise acquisition date > line_#.XTF.
 - b. Choose New Volume(F:) > 5-mile > “Survey Date” > “line_#.XTF”. This will initiate playback of line_#.XTF.
2. Two “waterfall” windows will appear. The active window will be highlighted “blue” and this is the frequency in which geometric and radiometric corrections will be applied. Right clicking the mouse button in the active “waterfall” will display the channels, which are being played back. Channels 1 and 2 are the port and starboard channels for the 100 kHz frequency and channels 3 and 4 are the port and starboard for the 500 kHz (384 kHz).

- a. Typical setup: Channel 1 & 2 selected in 100 kHz, Channel 3 & 4 in the 500 kHz, 100 kHz window highlighted.
 - b. To replay the file again: go to FILE > PLAYBACK and repeat #1.
 - c. Slow or speed up the playback by selecting the “walking guy” or “running guy” on the toolbar.
3. Survey tracks for this project were obtained using minimal overlap between adjacent lines. To ensure full coverage when constructing the final mosaic, the range scale over which data is processed needs then to be maximized.
 - a. In VIEW > DEPTH, DELAY, DURATION use the slider bar to set duration to range between 100.98 - 106.36 m. This change will be reflected in the “waterfall” window.

Setting Bottom Tracking Parameters

1. In VIEW > OVERLAY check on/off “show bottom track” also known as “first signal return.” This parameter is a detection of the seabed directly below the towfish and calculates the fish height. It is important for correcting errors due to slant range.

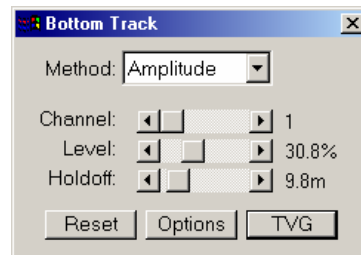
- a. Typical settings:

Method: Amplitude

Channel: 1

Level: data dependent (range = 10 - 35%).

Holdoff: data dependent (range = 8 - 14 m).



- b. Parameters should be modified such that the red first signal return line is coincident with the contact between water column and bottom return. Replay file modifying above parameters until satisfactory.

Slant-Range and Speed Correction

1. Correcting for errors due to slant range involves geometrically repositioning sonar data to counteract the effects of range data compression. Correcting for slant-range also removes the water column from the record. Speed correction coordinates the speed of the survey vessel to the length of the sonar record.

- a. Right click on “waterfall” window for each separate frequency. In the “waterfall display” window check off correct for slant-range and speed. Replay file to ensure that water column has been removed.

Set Time Varying Gain (TVG) Parameters

1. This application along with “Balance” are used to equalize returns across track in order to maintain an even image across the sonar record otherwise affected by attenuation. In order to modify TVG, the voltage distribution across the swath must be viewed. Go to WINDOW > SIGNAL > VOLTAGE ACROSS. Right click on the VOLTAGE WINDOW to make sure the 100 kHz signals are visible (1, 2). Manipulate windows so they cascade vertically. Optimal result is one where voltage is relatively equal across entire swath.

- a. Typical settings:

Channel: All

Standard: Off

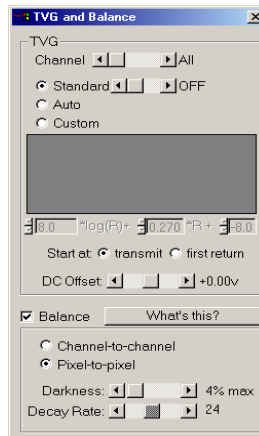
Start at: Transmit

DC Offset: +0.00 v

Balance: On (✓)

Darkness: 4% Max

Decay Rate: 24



Creating the Mosaic

1. In TOOLS > COVERAGE MAP AND MOSAIC OPTIONS check “Full DelphMap mosaic.” This will initiate opening of the “Delph Mosaic and DTM” window. Click “set projection and bounding box.”

- a. Typical map and projections settings:

Resolution: 0.25 m

Depth: < 2000 m

Units: dd.dddd

Output Projection: Universal Transverse Mercator, Zone 18

Datum = WGS Datum (1984)

- b. Under “more options” check “apply nav from mosaic and enter setup. Choose “compute layback from cable out,” check off “cable out.” Enter the following typical settings and “apply” the changes.

Cable Out: 15 m

Offset: 11 m

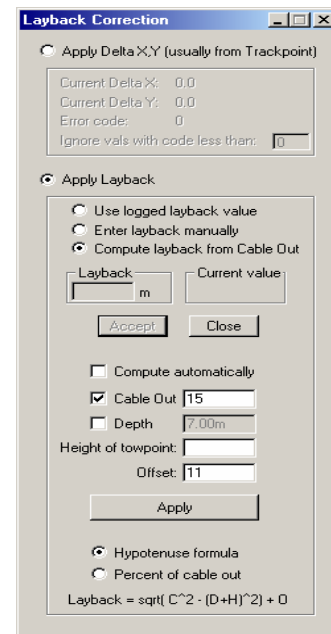
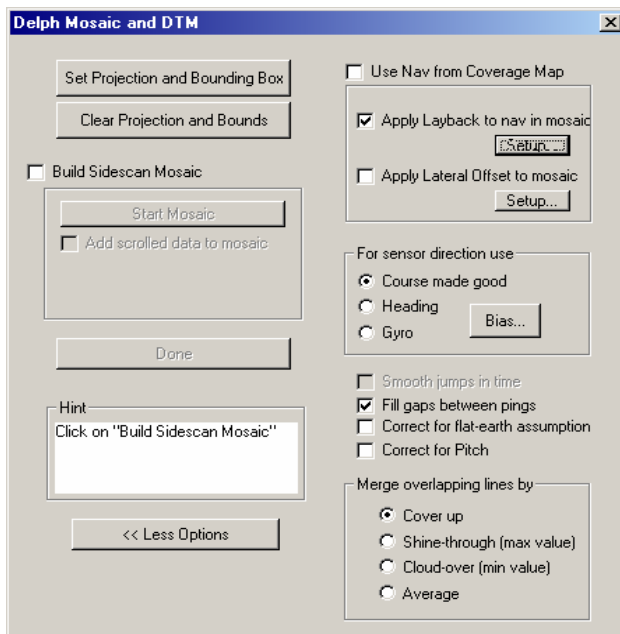
Hypotenuse Formula: On

- c. Other setup options:

For sensor direction use: Course made good

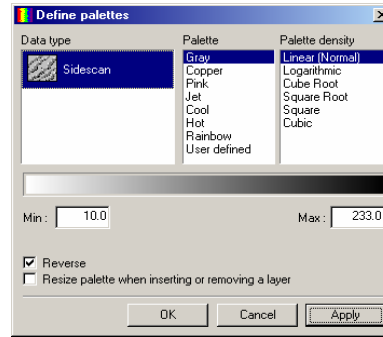
Fill gaps between pings: On

Merge overlapping lines by: Cover up

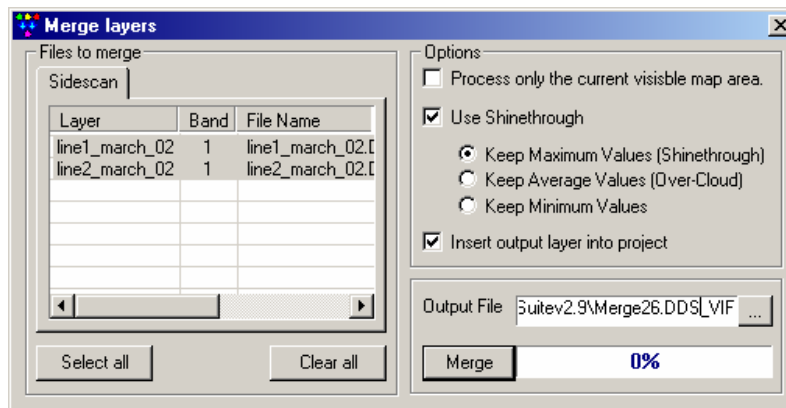


- Return to “Delph Mosaic and DTM” window and click on “Build Sidescan Mosaic.” Click on “Start Mosaic” to specify mosaic file name. Save file as a geonoded file with *.DDS_VIF tag. Once “save” has been clicked, return to “Isis Main Window” and playback the line to be mosaicked.
- Open *DelphMap v2.9* and import processed lines accordingly. Under GIS Tools > Color Palettes make the following modifications. Gray shade pixel values are reversed to highlight high-energy backscatter returns as black and lower energy returns with correspondingly lighter colors fading to white.

Data Type: Sidescan
 Palette: Gray
 Palette Density: Linear (normal)
 Minimum: 10
 Maximum: 233
 Reverse: On



4. After all lines have been inserted into *DelphiMap* merge individual lines are merged into one large mosaic file. This is appropriate for a regional view of surveyed area and to observe large-scale features on the seabed. For applications used in this research, lines were exported individually to be georeferenced relative to one another and limit navigation errors inherent in sidescan acquisition.
 - a. To create mosaic go to TOOLS > MERGE IMAGE LAYERS and use the following settings:
 Use Shinethrough: on
 Keep Maximum Values (Shinethrough): On
 Insert output layer into project: On



- b. To georeference individual lines relative to each other:
 - i. Using *DelphiMap* export individual lines from a given survey as geotiff image files with the *.TIFF tag. In doing so, a secondary file (*.tfw tag) is created containing the necessary geographic information needed to place this image in it's proper space in a given coordinate system. This

header file, also known as a world file consists of the upper left-hand corner coordinates of the image as well as current pixel resolution.

- ii. Use a GIS software package to view individual lines. *ARCVIEW* 3.2 was used in this research.
- iii. Choose a well-defined benchmark that preferably runs perpendicular to multiple lines. Manipulate coordinates given in the world file to move the mosaic in space until the chosen fixed point is aligned across the lines. Repeat with other fixed features as needed. For purposes presented here, this method established a higher degree of confidence in analyses of temporal changes of sediment boundary locations across repeat mosaics of the same area.

Appendix C: Instructions for Calculating Sand Body Displacement

1. Open *ArcView 3.X*. Go to File>Extensions and turn on *XTools* extension script.
 - a. *XTools* defaults used in this study are as follows:
 - Map Units: meters
 - Output Map Units: Meters
 - View Distance Units: Meters
 - Area Output Units: Both acres and hectares
 - Convert overlay output shapes to single point: No
 - Calculate Area, Perimeter, Acres, Length: Yes
 - Do NOT show View Properties: Off
 - Do NOT show the XTools Default: Off
 - Projection: none

2. Digitize Sand Body
 - a. Select “Draw Polygon” feature from the toolbar and digitize the perimeter of the chosen sand body. This will create a new “graphic” shape.
 - b. To convert graphic to shape file go to XTools>Convert Graphics to Shapes.
 - c. Go to Edit> Delete Graphics and then turn on the newly formed “sandbody1.shp” file to view.
 - d. Repeat for same sand body from subsequent survey date.

3. Calculate Intersection
 - a. Go to XTools>Intersect Themes. Select the two newly created “sandbody.shp” files to be intersected and choose a new a new output theme name.
 - b. Turn on the newly formed “intersection.shp” file to view.

4. Calculate Individual Area
 - a. Go to XTools>Calculate Area, Perimeter, Length, Acres, Hectares.
 - b. Select the newly formed “intersection.shp” file to calculate the area in square meters.

- c. Repeat for the “sandbody.shp” files from each chosen survey.
 - d. To obtain the area in square meters, first make the theme you wish to observe active. Select the “identify” tool on the toolbar. In the “View” window click on the region coincident with the active theme and the area statistics will be displayed.
5. Calculate Displacement Area
- a. Sum the “individual areas” of the two sand bodies. Divide this number by two to obtain the average size of the sand body over the period.
 - b. Subtract the “area of intersection” from the above to obtain the area of displacement in square meters.
 - c. Overlay the sand bodies to determine direction of displacement.

Appendix D: Change detection analysis results of selected lower sand flat sand bodies.

| CSB #1 Sample Date | Coarse Sand Area (m ²) | Displacement & Direction from Spring '02 (m ²) | Displacement & Direction from Fall '02 (m ²) | Displacement & Direction from Spring '03 (m ²) | Displacement & Direction from Fall '03 (m ²) |
|--------------------------|---|--|--|--|--|
| Spring '02 | 4775 | n/a | 315 ND | X | 413 ND |
| Fall '02 | 4477 | 315 ND | n/a | 438 W-NW | X |
| Spring '03 | 3870 | X | 438 W-NW | n/a | 490 E |
| Fall '03 | 4449 | 413 ND | X | 490 E | n/a |

Results from change detection analysis of Coarse Sand Body #1.

ND – no net directional component X - not recorded n/a - not applicable

| CSB #2 Sample Date | Coarse Sand Area (m ²) | Displacement & Direction from Spring '02 (m ²) | Displacement & Direction from Fall '02 (m ²) | Displacement & Direction from Spring '03 (m ²) | Displacement & Direction from Fall '03 (m ²) |
|--------------------------|---|--|--|--|--|
| Spring '02 | 1731 | n/a | 233 ND | X | 180 N |
| Fall '02 | 1420 | 233 ND | n/a | 257.27 ND | X |
| Spring '03 | 1666 | X | 257 ND | n/a | 152 N-NE |
| Fall '03 | 1748 | 180 N | X | 152 N-NE | n/a |

Results from change detection analysis of Coarse Sand Body #2.

ND – no net directional component X - not recorded n/a - not applicable

| FSB #1 Sample Date | Fine Sand Area (m ²) | Displacement & Direction from Spring '02 (m ²) | Displacement & Direction from Fall '02 (m ²) | Displacement & Direction from Spring '03 (m ²) | Displacement & Direction from Fall '03 (m ²) |
|--------------------------|---|--|--|--|--|
| Spring '02 | 321 | n/a | 63 ALL ≠ N/NE | X | 120 N-NW |
| Fall '02 | 421 | 63 ND | n/a | 146 N-NW | X |
| Spring '03 | 386 | X | 146 N-NW | n/a | 46 SE |
| Fall '03 | 329 | 120 N-NW | X | 46 SE | n/a |

Results from change detection analysis of Fine Sand Body #1.

ND – no net directional component X - not recorded n/a - not applicable

| FSB #2 Sample Date | Fine Sand Area (m ²) | Displacement & Direction from Spring '02 (m ²) | Displacement & Direction from Fall '02 (m ²) | Displacement & Direction from Spring '03 (m ²) | Displacement & Direction from Fall '03 (m ²) |
|--------------------------|---|--|--|--|--|
| Spring '02 | 3386 | n/a | 312* ND | X | 443 ND |
| Fall '02 | 3478* | 312* ND | n/a | 545* N | X |
| Spring '03 | 4087 | X | 545* N | n/a | 588 ND |
| Fall '03 | 3805 | 443 ND | X | 588 ND | n/a |

Results from change detection analysis of Fine Sand Body #2.

Asterisk (*) denotes loss of NE corner of data due to nadir region.

ND – no net directional component X - not recorded n/a - not applicable

| FSB #3 Sample Date | Fine Sand Area (m ²) | Displacement & Direction from Spring '02 (m ²) | Displacement & Direction from Fall '02 (m ²) | Displacement & Direction from Spring '03 (m ²) | Displacement & Direction from Fall '03 (m ²) |
|--------------------------|---|--|--|--|--|
| Spring '02 | 2603 | n/a | 478 S-SW | X | 538 W |
| Fall '02 | 3532 | 478 S-SW | n/a | 384 ND | X |
| Spring '03 | 3566 | X | 384 ND | n/a | 540 ND |
| Fall '03 | 2490 | 538 W | X | 540 ND | n/a |

Results from change detection analysis of Fine Sand Body #3.

ND – no net directional component

X - not recorded

n/a - not applicable

| FSB #4 Sample Date | Fine Sand Area (m ²) | Displacement & Direction from Spring '02 (m ²) | Displacement & Direction from Fall '02 (m ²) | Displacement & Direction from Spring '03 (m ²) | Displacement & Direction from Fall '03 (m ²) |
|---------------------------|---|---|--|--|--|
| Spring '02 *over nadir | 12816* | n/a | 1378 ND | X | 869 ND |
| Fall '02 *over nadir | 14717* | 1378ND | n/a | 750 ND | X |
| Spring '03 *over nadir | 13842* | X | 750 ND | n/a | 832 ND |
| Fall '03 *over nadir | 12779* | 869 ND | X | 832 ND | n/a |

Results from change detection analysis of Fine Sand Body #4.

ND – no net directional component

X - not recorded

n/a - not applicable